AN INVESTIGATION OF THE ENERGY BALANCE OF A TUBE SOLARIMETER.

By Wilson Kipkoech Ng'etich

A thesis submitted as partial fulfillment for the degree of Master of Science of the University of Nairobi.

1990

DECLARATION

This thesis is my original work and has not been submitted for examination in any University.

Date

Ng'etich, W.K. _____ 8/5/90

I/56/7646/87 Department of Physics
University of Nairobi

This thesis has been submitted with our approval as university supervisors

Date

Prof. W. H. Drake. _____ 13/6/90
Department of Physics
University of Malawi
Malawi

Dr. C. L. Coulson. _____ 27/5/90
Department of Botany
University of Nairobi
Kenya

Prof. C. J. Stigter. _____ 27/5/90
Department of Meteorology
Agricultural University
Wageningen
The Netherlands

ACKNOWLEDGMENTS

I wish to express my profound gratitude to my supervisors, Prof. Drake for his constant help, guidance and encouragement; Dr. Coulson for whose ideas gave rise to the project and Prof. Stigter for his help in the theoretical background of the work and use of TTMI equipment.

I would also like to thank Mr. Mungai of Department of Geography for enlightening conversations and useful suggestions. The technicians in the department of Physics for their help in acquiring various equipments and components. Mr. Musyoki of Department of Crop Science for his assistance and advice. Mr. Bates of ODA microcomputer project for technical advice.

Lastly I would like to thank all those who in one way or another contributed to the completion of this project.

CONTENTS Page

LIST OF FIGURES AND TABLES

List of Symbols and abbreviations

A,B,C ... used in equations are constants.

R_n - net radiation

P_b reflection coefficient

L_b - full black body radiation

L_d - long wave radiation flux from atmosphere

L_e - long wave radiation flux from surroundings

σ - is the Stefan's constant

k - thermal conductivity

C_p - specific heat

ϵ is the emisivity

T is temperature

T_b - surface temperature

S_t is the direct and diffuse radiation from the sky

S_e is the sunlight reflected from the surroundings.

TC thermocouple

ϕ , β are angles

TTMI - Traditional Techniques in Microclimate Improvement. This is a project under Prof. Stigter of the Department of Meteorology, Agricultural University, Wageningen, The Netherlands.

BBC - British Broadcasting Corporation. This is a brand name of the computer used in the project.

DTT - Digital Thermocouple Thermometer. This is a digital instrument used in the project for temperature measurements.

P.A.R. - Photosynthetically Active Radiation

V.I.A. - Versatile Interface Adapter

S.W.G. - Standard Wire Gauge

Multiplexer - This is a channel selector with a logic switch. The switch is controlled by digital signals e.g. from a computer.

Counter - This is a binary counter which outputs a binary number (i.e either 1 or 0) when under the influence of a clock pulse.

A clock pulse is the change of state in a digital signal for one period.

Buffer - This is basically a booster for TTL signals and well as providing signal isolation.

TTL - Transistor - Transistor Logic.

Gate - This is a logic 'decision box' which outputs certain value(s) given certain input(s).

ABSTRACT

Results of an investigation of the energy balance of a tube solarimeter are presented. Tube solarimeters appear to be affected by various tropical conditions which might prevail in the field. High ambient temperatures (typically about over 40^{o}C) and high solar radiation loads increases, under conditions of low wind speeds, the output ratio of a tube solarimeter with a Kipp solarimeter reference by between 8% and 17%. Mild condensation increases this output ratio of a tube solarimeter by up to 4% as compared to one without condensation and the percentage is even higher with more serious condensation. Wind speed increases the rate of cooling of the tube solarimeter significantly and hence an improvement of the response time of the instrument occurs. An influence of apparent sky temperature could only be hinted at but could not be determined quantitatively. The trend of the errors encountered is the same as those from radiation geometry proven earlier to exist (Mungai, personal communication). An interface to input data from sensors (thermocouples) through a Digital Thermocouple Thermometer to a BBC microcomputer has been built. The data were analysed using INSTAT, a statistical package for the BBC microcomputer.

CHAPTER 1

1.INTRODUCTION

1.1 GENERAL

1.1.1 INTRODUCTION

Kenya's economy depends mainly on agriculture. Food production is influenced by many factors, among them light (quality and quantity) which is required for dry matter production through photosynthesis. Solar radiation is confined to 0.1 to 3μm waveband with the amount of energy being greatest at about 0.48μm. At a mean distance between the sun and earth of 1.5×10^8 km, the irradiance at right angles to the solar beam is known as the solar constant which is about 1360 W m^{-2}. The solar spectrum is divided into three regions: the ultra violet (0.1 to 0.4μm); the visible region (0.4 to 0.7μm) and the infra-red region (0.7 to 3μm). Of the total light spectrum only the "visible" light or the so called photosynthetically active radiation (PAR) is useful to the plants for photosynthesis. Measurements of PAR (0.4 to 0.7 μm) are necessary in determination of, for instance, photosynthetic efficiency, crop reflectance (can also be used for total), photosynthetic light interception etc.

In the visible (PAR) region of the spectrum, absorption by

atmospheric gases is much less important in determining the spectral distribution. In the infra-red region, however, absorption is more important than scattering and several atmospheric constituents absorb strongly, notably water vapour and water with absorption wavelengths 0.9 and 3μm. Presence of water vapour and water in the atmosphere then increases the amount of visible radiation relative to infra-red radiation. However, the PAR percentage of global radiation is relatively conservative because differences due to scattering and molecular absorption of PAR and non-PAR radiation tend to oppose each other (e.g. Stigter and Musabilha, 1982). Even for overcast skies this percentage is only about 25% higher than for clear or partly cloudy skies.

1.1.2 SOLAR RADIATION MEASUREMENTS AND INSTRUMENTATION

The most widely used instrument in solar radiation measurement is a pyranometer. This is a device which is sensitive to thermal radiation. It measures radiation by the temperature differential between two surfaces or a derived factor. It has a view angle of 2π steradians and measures global irradiance received on a horizontal surface. Because of the need to integrate over space, long detectors are necessary such as tube solarimeters. Also a

combination of several small sensors or moving sensors are used. Such detectors are useful where the spatial distribution is non-uniform e.g. below a canopy.

The spectral response of these tubes lies between wavelengths 0.35 to 2.5μm for "unfiltered" tubes. Gelatin filters with a cut-off above 0.7μm are filled in some radiometers and are used in the so called "filtered" tubes to measure only radiation above 0.7μm. The difference between the filtered and unfiltered tube solarimeters outputs represents the PAR.

Tube solarimeters are thermoelectric radiometers. They convert the absorbed thermal energy into an electrical signal via a thermopile, which is a number of thermocouples connected in series. The tube solarimeter thermopile measures the temperature differential between two differently coloured surfaces i.e black and white, surface arranged in an alternating pattern. This temperature differential is then expected to be directly proportional to the irradiance falling on the sensor.

Standard meteorological equipment are used for reference purposes. The Moll-Gorczynski pyranometer, such as manufactured by Kipp and Zonen, is often used as a sub-standard (e.g. Norris 1973). This also measures radiation

by temperature differential between the black surface and the protected, white painted, base of the instrument.

1.1.3 STATEMENT OF THE PROBLEM

In the tropics, where high diurnal variations in temperature and in solar and net radiation are experienced, tube solarimeters present a number of problems to the user. Some of these are:

1) Condensation - this occurs in the tube even when it had been flushed with dry air.

This problem has been encountered, among others, in an on-going research in the Traditional Techniques of Microclimate Improvement (TTMI) project (Coulson, Stigter, Mungai personal communication). It is known that even the smallest leak may eventually lead to patterns of condensation appearing in the tube (Delta-T Devices, 1984) The radiation reaching the thermopile is reduced by condensation droplets on the glass (by reflection, refraction and absorption) and since condensation appears and disappears, especially above the coldest (white) surfaces, the output from the sensor is liable to lower, hence an increase in the sensor output.

Condensation plays an important part in the heat balance of the tube, influenced by convection, and hence an

understanding of the condensation patterns is desirable.

2). Ambient temperature/wind speed. The tube solarimeter has a cylindrical pyrex (Borosilicate glass) cover (Delta-T Devices Ltd, 1984, Corning Ltd., 1981). Radiation absorbed by the sensor surfaces, more by the black than by the white ones, is partly re-radiated at longer wavelengths, which is then trapped inside the tube. At high external temperatures and low wind speeds this may increase the "greenhouse" effect in the tube, which in turn may induce changes in the output from the thermopile relative to a reference solarimeter. Thus high external temperatures and air movement changes at relatively low wind speeds may alter the sensor output. Since air temperature in the semi-arid tropical areas can be high (up to 40^{o}C) and since there are research situations when the tubes will be sited near the ground, where wind speed will be low, erroneous outputs could be common. The angle at which air movement strikes the tube may also be important. The heat transported between a heated cylinder and a fluid decreases from maximum when flow is normal to its axis, to a minimum when parallel to its length (Shaw *et al*, 1973). Such problems do not occur with reference pyranometers (solarimeters) with double glass protection,

where the "greenhouse effect" has already been minimised by better insulation.

1.2 INTRODUCTION TO RADIOMETERS USED IN THE RESEARCH

1.2.1 TUBE SOLARIMETER

The tube solarimeter consists of a copper-constantan thermopile, mounted on a surface with sections painted white or black, housed in a cylindrical pyrex glass tube of external diameter 2.62cm and a thickness of 1.5mm and is 1m long. The thermopile has sixty thermocouples on the surface, which is arranged in an alternating pattern of black and white per every ten thermocouples. This measures the temperature difference caused by differences in absorption of the incident radiant energy flux. Delta-T solarimeters are calibrated with a shunt resistor to give an output of 15mV per kW m^{-2} (Delta-T Devices Ltd., 1984). The functional diagram of the tube is shown in figure 1. The 99% time constant is approximately 3 minutes (Delta-T Devices Ltd.,1984). The thermal time constant of a sensor is defined as the time required for the sensor temperature to stabilize to environment temperature for a step change (Benedict, 1969) .

Figure 1.

a) Photograph of two tube solarimeters mounted perpendicular to each other. The white and black sections of the sensor element can be seen.

b) Functional diagram of a tube solarimeter. R_s is the resistance of the cable and sensor internal resistance, R_c is the shunting resistor and V_s is the source voltage produced by the thermocouples.

(a)

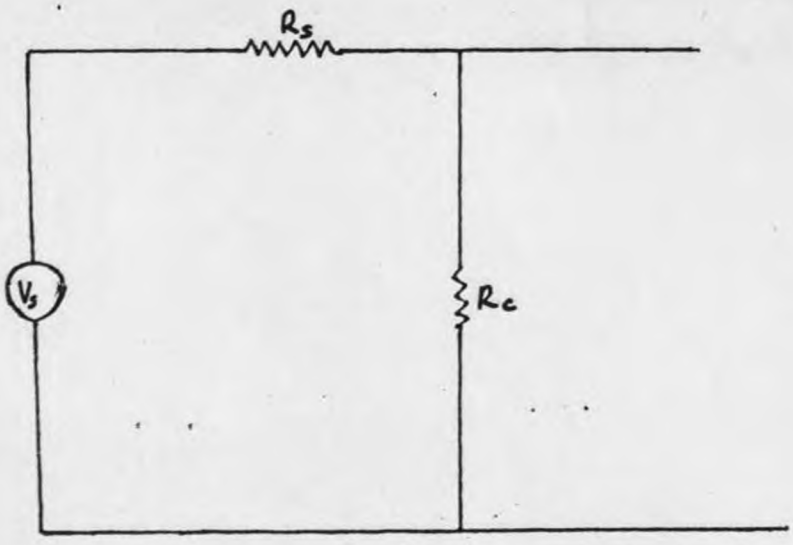

(b)

Figure 1

1.2.2 KIPP SOLARIMETER

This is also known as the Moll - Gorczynski pyranometer. It has a 14 - junction Manganin - constantan thermopile having a sensitivity of about 12μV $W^{-1}m^{-2}$, and a resistance of approximately 10 ohms, in the form of a 10 x 14 mm rectangle. The thermopile is flush with the edge of its brass case with which the cold junctions are in contact. The blackened surface of the thermopile is covered by two concentric, optically ground, glass hemispheres of 30 and 50 mm in diameter. The air space between the hemispheres, which provide thermal insulation , is usually connected to a bottle of desiccant to prevent condensation on the inner surfaces. The 98% time constant is about 30 seconds. The thermopile is not compensated and has a temperature coefficient of -0.2% per ^{o}C (Fritschen and Gay, 1979). The Kipp solarimeter used in the project had a calibration of 12.6mV $KW^{-1}m^{-2}$.

Figure 2.

Photograph of a Kipp solarimeter. The spherical glass domes housing the sensor element can be seen. The white screen plate is to keep the base of the solarimeter, in which the reference thermocouple is embeded, at constant temperature.

Figure 2

CHAPTER TWO

2. LITERATURE REVIEW

2.1 GENERAL.

Radiometer is the generic name for a range of devices that measure radiation by absorbing the radiation and converting it to thermal energy. Part of this thermal energy is then used in a form suitable for measurement, which may be an electrical signal (Woodward and Sheehy, 1980), although for solar radiation mechanical and distillation devices also exist. Most electrical solarimeters use thermocouples to measure the difference between a black surface and a reference temperature within the instrument or between two surfaces (with different selective properties of absorption). This temperature differential represents the global radiation (i.e. sun + sky radiation).

Other radiation measuring devices are photosensitive devices. These include photo-diodes, light dependent resistors, photo-voltaic cells etc. These instruments are sensitive only to the photon energy of solar radiation and hence are free from the heat defects described earlier. Their spectral response is usually in the visible region (i.e. 0.4μm to 0.7μm), hence these instruments would be appropriate in P.A.R. measurements. These instruments have,for example, been used in Infra-Red Gas

These instruments have,for example, been used in Infra-Red Gas Analysers, to measure the PAR falling on a leaf. There some limitations of such instruments in this type of work. The use of such instruments in crops suffer from spatial inhomogeneity because of the discreteness of the sensors. They can only be used for spot measurements; for spatial measurements an array of these discrete devices has to be used. Though PAR can be measured accurately using such instruments,they cannot provide any useful information on near or far infra-red radiation. Kipyegon (1989) investigated the use of photosensitive devices to measure solar radiation. In his approach he used a photodiode and a light dependent resistor. Results form his work show that photodiodes can be more sensitive to low light levels than a Kipp solarimeter, but at higher levels they get quickly saturated.

2.2 DESIGN AND CONSTRUCTION OF TUBE SOLARIMETERS.

Szeicz *et al.*, (1964) described the design and construction of the original tube solarimeter. The construction of the sensing element was by an electroplating technique. The sensing element of the solarimeter consists of three sections of tufnol, 28cm long and 0.19cm thick, in a 1m length of pyrex tubing of 2.32cm internal diameter. Each half section is wound

with about 100 turns of 42 Standard Wire Gauge, S.W.G. (0.01cm diameter) constantan wire and at the center of the section, the wire is taken through a small hole to reverse the direction of winding. This reverses the position of 'hot' and 'cold' junctions with respect to the central axis. The copper is then deposited on three quarters of each turn by electroplating. The constantan wire to stay un-plated runs from the center of the black area to the center of the white area. This is shown in figure 3a.

Delta-T Devices Ltd., UK in collaboration with Prof. J.L. Monteith, produces the tube solarimeters commercially. These are available in two sizes: large - this is one meter long (TSL)-and miniature, which is 0.3m long (TSM). The TSL tube which was used in this investigation has sixty thermocouples on the sensor plate. This is housed in a pyrex glass which transmits, as said earlier, radiation of wavelengths .35μm to 2.5μm. The cosine response is an important feature of cylindrical radiation measuring instruments. Lang (1977) gives a theoretical review on the cosine effect of the tube solarimeters.

The Lambert cosine response is given by

$$C = [V(\beta=0)/V(\beta)]\cos\beta = 1 \qquad (1)$$

Figure 3.

(a) Diagram showing thermocouple windings in tube solarimeter. At the junction of the two sections, the winding is reversed. One half of each section is painted black and the other half white.

b) Diagram of a section of a tube solarimeter showing the cylindrical glass cover and the sensor element.

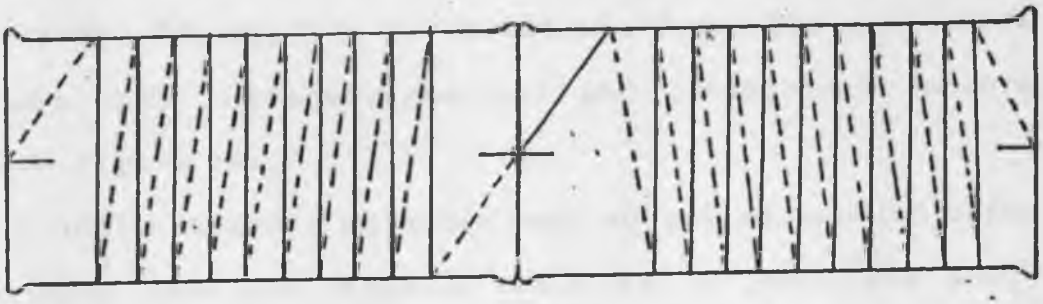

(a)

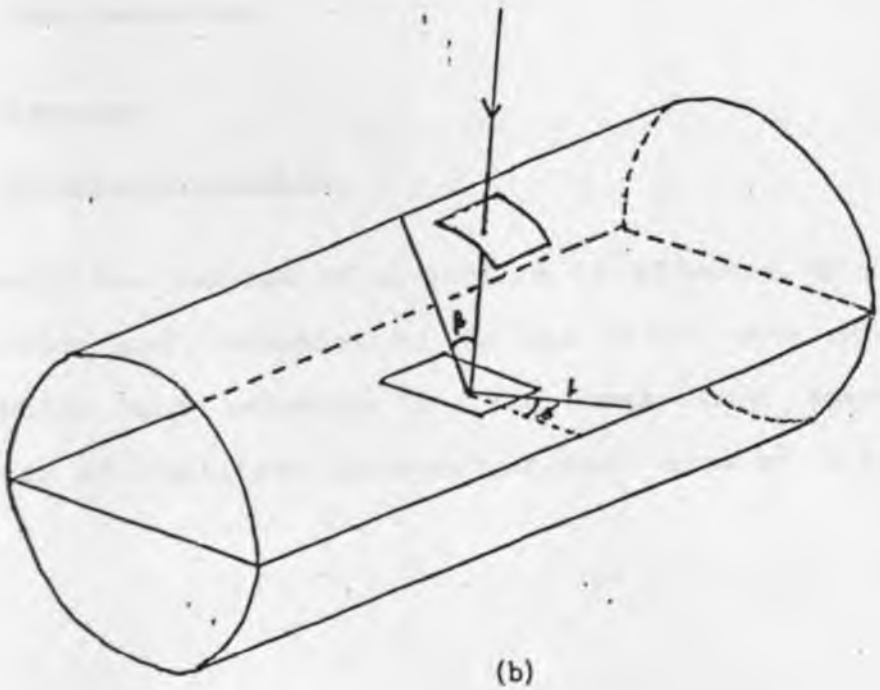

(b)

Figure 3

where V(β) is the output of the radiometer at a zenith angle β and V(β = 0) is the output at normal incidence (Woodward and Sheehy, 1980). Ideally C = 1, deviations from this are cosine errors and occur in hemi-spherical and cylindrical sensors (see also figure 3b).

In cylindrical sensors, an additional so called azimuth error occurs, which does not normally occur or is small for hemi-spherical sensors. As azimuth angle ø varies, L also varies, hence the energy received per unit area from that direction , which due to interaction with the glass, depends on ø, β and L also varies. This complicates response from cylindrical sensors, which become azimuth dependent. North/ South mounting of solarimeters therefore gives a different response from the East/ West mounting.

2.3 Theories

2.3.1 Radiation balance.

The radiation balance of a surface is affected by absorption, reflection and transmission in the short wave spectrum and absorption and emission in the long wave spectrum. The equation of radiative balance per unit area of a surface can

be written as:

Net radiation = [incident short wave radiation + absorbed long wave radiation] - [reflected and transmitted short-wave radiation + emitted long wave radiation]

This can be expressed symbolically as:

$R_n = (1 - p_b)(S_t + S_e) + \epsilon(L_d + L_e - L_b)$

where R_n is the net radiation per unit area of a body,

S_t is the direct and diffuse radiation from the sky

S_e is the sunlight reflected from the surroundings. Hence the total incident short wave radiation is $S_t + S_e$

p_b is the reflection coefficient of a body. Hence the absorbed short-wave flux is $(1-p_b)(S_t + S_e)$.

L_d is the long wave radiation flux from the atmosphere, which comes largely from the lowest 100m, L_e is this flux from the surroundings,

$L_b = \sigma T_b^4$ is the full black body flux of radiation at a (mean) surface temperature, T_b. Hence a surface with an emissivity of ϵ will gain $\epsilon(L_d + L_e)$ from its surroundings and emit ϵL_b to its surroundings (Monteith, 1973).

All natural materials reflect and transmit solar radiation in wave band from 0.4 to 3μm. Reflectivity is defined as the fraction of incident solar radiation reflected at a specific wavelength. Reflection coefficient is the average reflectivity

over a specified waveband, weighted by the distribution of radiation in the solar spectrum. Water vapour absorbs at waveband 0.9 to 3μm. Reflectivity of the soil depends, among other things, on the amount of organic matter. It usually increases with increasing wavelength and reaches a maximum between 1 and 2μm. Presence of water changes this to between 1.45 and 1.95μm. The reflectivity decreases as it gets wetter because radiation is trapped by internal reflection at air - water interfaces.

If a horizontal surface, O_2, is above a soil or other surface, O_1, with reflection coefficient p_1 it instantaneously receives an additional income of short-wave radiation $S_e = p_1 S_t$ and of long wave radiation $L_e = \epsilon_1 \sigma T_1^4$, when ϵ_1 and T_1 apply to O_1. The net radiation is therefore

$$R_n = (1 - p_2)(1 + p_1)S_t + \epsilon_2 L_d + \epsilon_2 L_e - \epsilon_2 \sigma T_2^4$$

where p_2 is the reflection coefficient of the horizontal surface O_2, T_2 is the temperature of O_2, ϵ_2 the long wave emission of O_2. Note that R_n is the net radiation of total surface area. For an actual energy balance of a tube, upper and lower sides are different. In most cases ϵ_1 and ϵ_2 may be taken as unity.

2.3.2 Heat conduction.

Cylindrical systems often experience temperature gradients in the radial direction only and hence can be treated as one dimensional. However, tube solarimeters have temperature gradients also along the tube because of the different material (i.e. the plastic ends) attached to its ends. Heat conduction occurs from inside to outside of the cylinder in the case of $T_{inside} > T_{outside}$ (see figure 5).

The rate at which heat is conducted across any cylinder of finite length l, thermal conductivity k and radius r is given as;

$q_r = -kAdT/dr = -k(2\pi rl)dT/dr$

which when solved gives

$q_r = 2\pi lk(T_{s1} - T_{s2})/\ln(r2/r1)$.

Note q_r is independent of r.

The temperature distribution at any point r is given as

$T(r) = (T_{s1} - T_{s2})/\ln(r1/r2) \times \ln(r/r2) + T_{s2}$ (3)

(Incropera, 1981).

Fig. 4. Diagram of a cross-section of hollow cylinder, of inner radius r_1 and outer radius r_2. The temperature of the inner surface is denoted as T_{s1} and of the outer surface as T_{s2}.

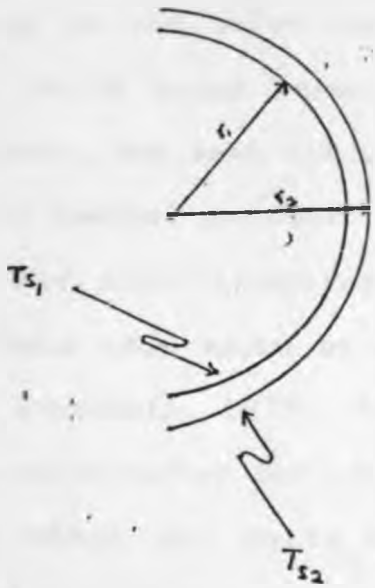

Figure 4

2.3.3 Convection

Convective heat transport is defined as an indirect form of heat transport. Radiation and conduction are regarded to be the only basic heat flow processes. Convection typically involves heating a small mass of fluid at or near a surface, mainly by conduction in the case of air, and therefore increasing its internal energy. In the case of the warmer mass being in and below the colder mass, free convection occurs, which mixes warmer masses among colder ones. In other cases, the mass circulates into the bulk of the fluid due to general movement (laminarily or by forced convection) and also transfers its excess internal energy to the bulk once again by conduction and divergence of radiation (Cornwell, 1977). Free convection is caused in the tube solarimeter by the temperature difference between the black and white surfaces. The movement of fluid in free convection results from buoyancy forces imposed on the fluid when its density in the proximity of the heat transfer surface is decreased as a result of the heating process. Gases (including air) offer the greatest resistance to heat flow by conduction. However, they allow a considerable heat transfer by free

and forced convection, and over large distances and also radiation divergence, so that the heat conveyed by thermal conduction is, once away from the surface, only a small fraction. Natural free convection is the one we are concerned with inside the tube in two ways, cross-sectional and longitudinal, because temperature differences also exist in the horizontal on larger scale. A mixture of the two convective heat transport systems is applicable to the outer glass surface of the tube solarimeter at lower wind speeds.

CHAPTER THREE

MATERIALS AND METHODS

3.1 EXPERIMENTAL DETAILS

3.1.1 Fabrication and calibration of thermocouples

Due to unavailability of sufficiently thin thermocouples, it was decided to fabricate them. These were of type T (copper-constantan) with S.W.G 42 i.e diameter of 0.01cm which were fabricated using an arc-welding technique (Coulson, personal communication). A power supply was connected as shown in figure 6.

By passing a current of 1.4 Amps at 15 Volts and touching the pencil lead to a junction of the two wires, a good joint was made.

Calibration of thermocouples was done and compared to RS type-T thermocouples data. The thermocouples were calibrated using constant boiling temperature compounds : these were ice, methanol, Carbon Tetrachloride and water with boiling temperatures; $0^{o}C$, $60^{o}C$, $70^{o}C$ and $92.5^{o}C$ respectively. The thermocouples were left to hang just above the boiling liquid and the vapour temperature taken as the boiling temperature of the solution, except for ice in which the sensor was immersed.

Figure 5. Diagram showing the fabrication of the thermocouples. One end of the leads from the power supply was connevted to a pencil lead and the other connected to a twisted pair of constantan/copper wires.

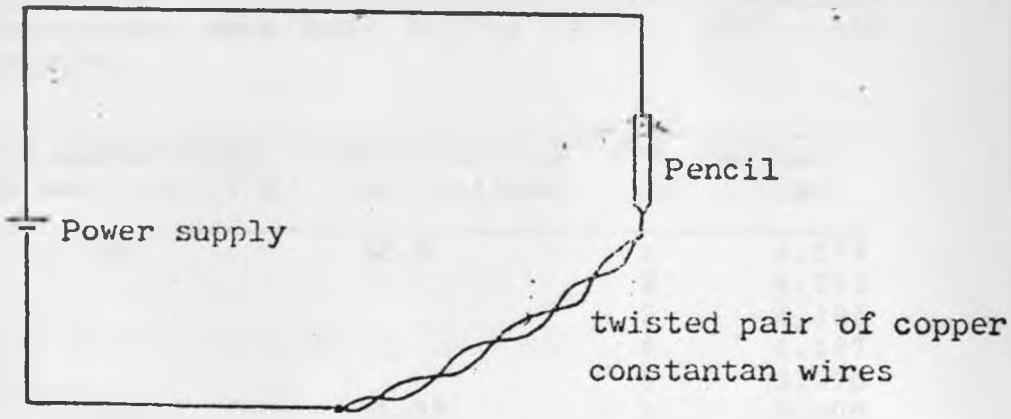
Pencil
Power supply
twisted pair of copper
constantan wires

Figure 5

The thermocouple equation was then applied to the calibration to get the calibration equations shown below: The thermocouple equation is:

$$E = AT + BT^2 + CT^3 + \ldots \quad (4)$$

Table I

Data on calibration of fabricated thermocouples. Reference of the thermocouples were kept in ice ($0^{\circ}C$). TC1 - TC5 are thermocouples.

Solution	Boiling/Melting at sea level ($^{\circ}C$)	Corrected for for Altitude	T/C No.	Output in mV
Water	100	92.9	1	4.178
			2	4.213
			3	4.195
			4	4.187
			5	3.910
Carbon Tetrachloride CCL_4	76.8	71.38	1	3.200
			2	3.149
			3	3.196
			4	3.201
			5	3.072
Methyl Alcohol	64.7	60.13	1	2.606
			2	2.601
			3	2.625
			4	2.600
			5	2.433

Where the terms A,B,C,.. are constants depending on the characteristics of thermocouple.

The corrected boiling points were calculated using the

pressure of Nairobi (706 mmHg) and using the equation:

$$PV/T = \text{Constant} \qquad (5)$$

Using the above results and the thermocouple equation, the following calibration equations were obtained with reference to ice, where higher terms of equation were neglected.

TC_1 $\quad E = 40.43T + 0.0566T^2 \qquad (6a)$

TC_2 $\quad E = 40.0956T + 0.0563T^2 \qquad (6b)$

TC_3 $\quad E = 40.575T + 0.068T^2 \qquad (6c)$

TC_4 $\quad E = 40.162T + 0.0956T^2 \qquad (6d)$

TC_5 $\quad E = 37.7T + 0.047T^2 \qquad (6e)$

TC_5 is a rolled constantan-manganin thermocouple, which has a sensitivity of about 40 $\mu V/^oC$ at 20^oC (Stigter, personal communication). In these thermocouples, the junction between constantan and manganin is flattened instead of a bead like in other thermocouples. This flattened junction gives better surface contact with glass matterial. The Copper-Constantan thermocouples used have a sensitivity of about 42 $\mu V/^oC$ (RS catalogue 1987). Figure 7 show a comparison between the thermocouples made and data from RS catalogue on copper/constantan thermocouples (RS data sheet 4793, July 1985). The cause of the

Figure 6.

Graph of thermocouple output comparison. o—o data from TC_1. _____ is data from RS catalogue 1987.

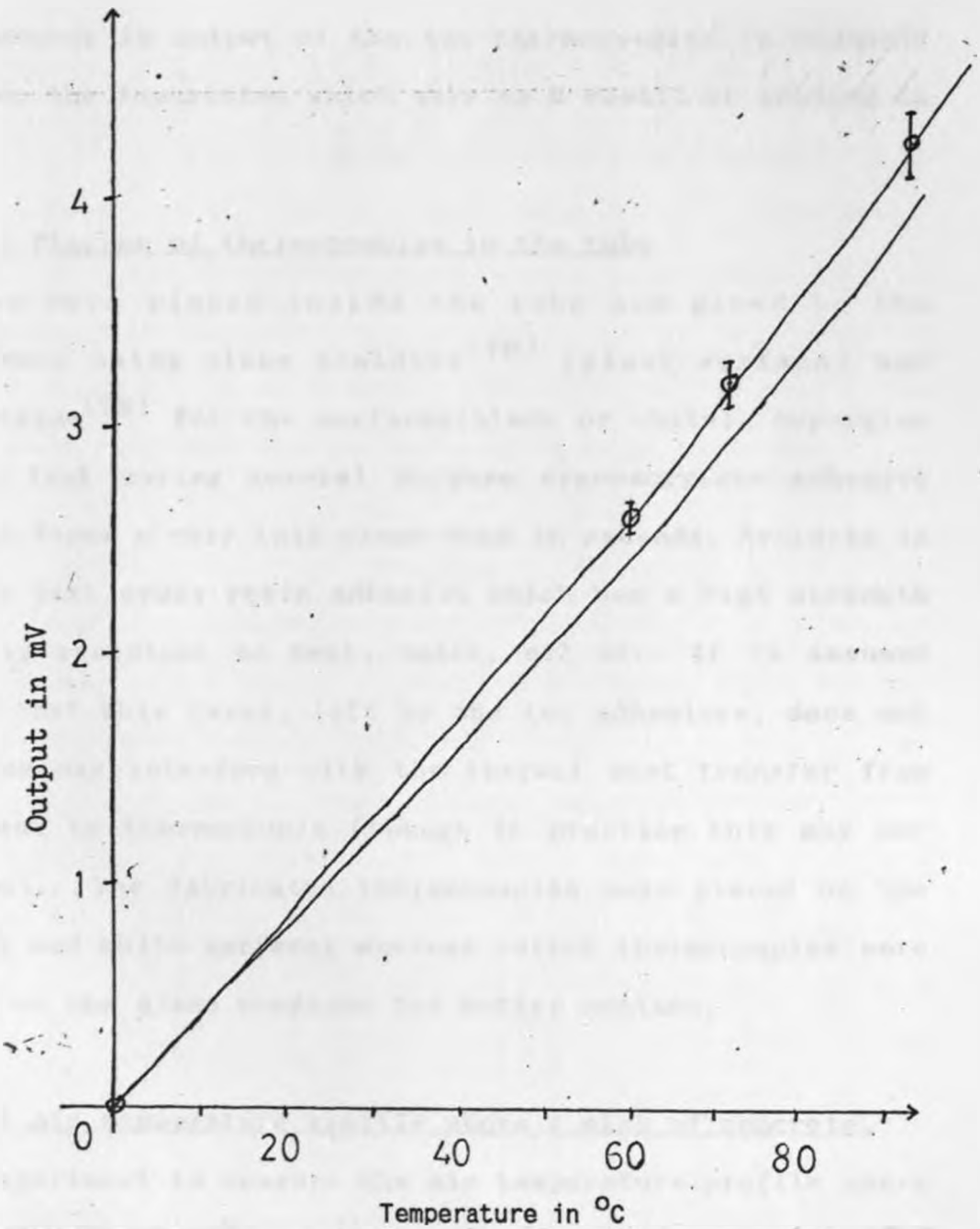

Figure 6

difference in output of the two thermocouples is probably due to the impurities which were as a result of welding in air.

3.1.2 Placing of thermocouples in the tube

These were placed inside the tube and glued to the surfaces using clear Araldite(TM) (glass surface) and superglue(TM) for the surfaces(black or white). Superglue is a fast curing general purpose cyanoacrylate adhesive which forms a very thin clear bond in seconds. Araldite is a two part epoxy resin adhesive which has a high strength and is resistant to heat, water, oil etc. It is assumed here that this layer, left by the two adhesives, does not in any way interfere with the thermal heat transfer from element to thermocouple (though in practice this may not be so). The fabricated thermocouples were placed on the black and white surfaces whereas rolled thermocouples were used on the glass surfaces for better contact.

3.1.3 Air temperature profile above a slab of concrete.

An experiment to measure the air temperature profile above a slab of concrete on the roof, where the experiments took place ,was done to determine the maximum air temperatures inside a windshield and the best height of a

tube solarimeter under this situation. The results are presented in table II below. With the presence of a windshield, the temperature profile followed an exponential curve (figure 7 and table II), as expected , with temperature changes reducing with increase in distance from the concrete. A similar curve was found to exist without a windshield though the temperature difference between the surface and 1m high was lower.

Table II

Comparison of temperature profiles above a slab of concrete in open air and inside polythene windshield. air1 and wind1 refers to air temperature and wind speeds respectively, measured in the open and air2 and wind2 are measurments inside windshield.

Height (cm)	air1 (^{o}C)	wind1 (m/s)	air2 (^{o}C)	wind2 (m/s)
0	37.8	0.08	36.9	0.86
10	35.7	0.10	35.0	1.04
20	33.8	0.14	30.1	1.33
30	32.6	0.22	28.5	1.16
40	31.9	0.20	28.2	1.35
50	31.5	0.28	26.8	1.83
60	31.1	0.25	26.3	1.74
70	30.8	0.26	26.5	0.98
80	30.3	0.37	25.8	0.47
90	30.1	0.29	25.1	2.00

It can be concluded that the temperature gradient has appreciably reduced at 1m height above the concrete

Figure 7.

Graph of air temperature profile within a polyth
windshield. The data was obtained using a Lambretch 64

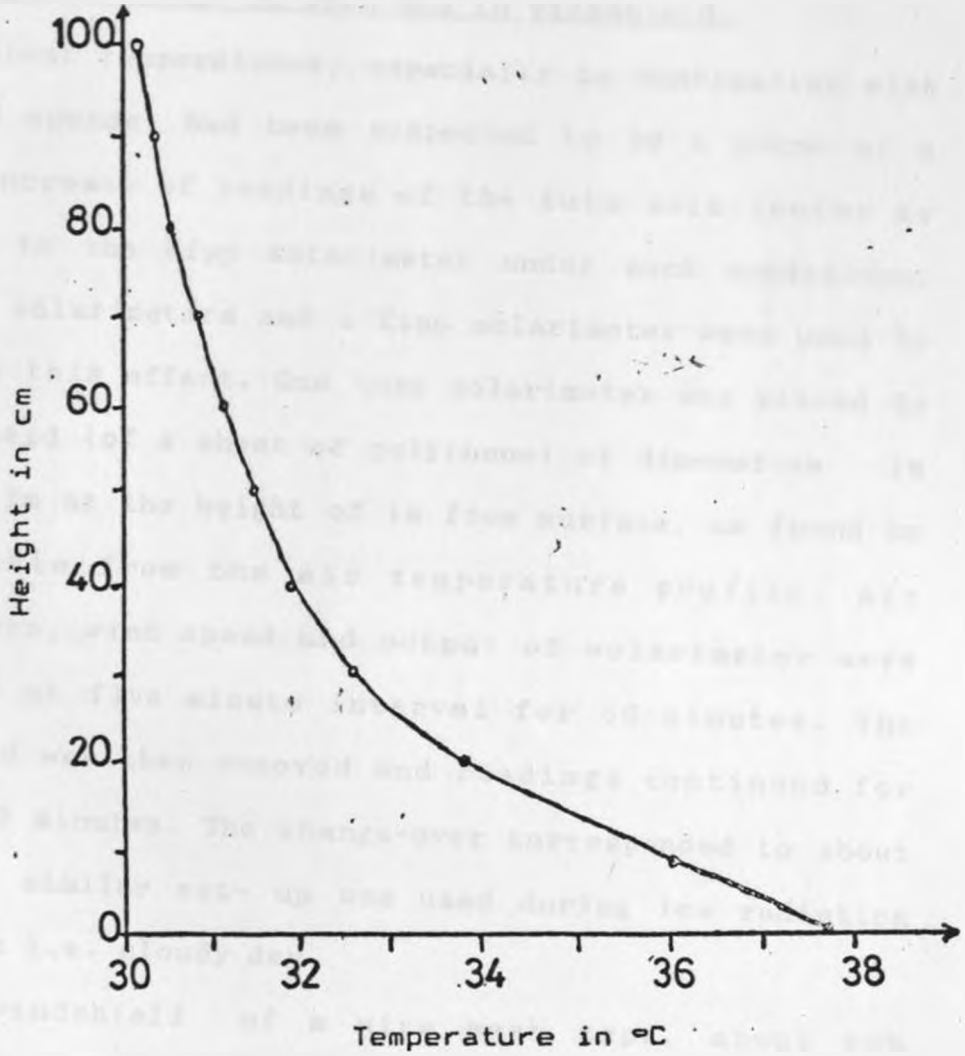

Figure 7

surface. Hence this was the height of the tube solarimeter used throughout the experiment.

3.1.4 Output of tube in open and in windshield.

High ambient temperatures, especially in combination with low wind speeds, had been suspected to be a cause of a larger increase of readings of the tube solarimeter as compared to the Kipp solarimeter under such conditions. Two tube solarimeters and a Kipp solarimeter were used to determine this effect. One tube solarimeter was placed in a windshield (of a sheet of polythene) of dimensions 1m x 1.5m x 1m at the height of 1m from surface, as found to be suitable from the air temperature profile. Air temperature, wind speed and output of solarimeter were monitored at five minute interval for 50 minutes. The windshield was then removed and readings continued for another 50 minutes. The change-over corresponded to about midday. A similar set- up was used during low radiation conditions i.e. cloudy day.

Using a windshield of a wire mesh type, about 60% permeable , no change in the output of the tube/Kipp ratio was noticed during high radiation load (i.e. comparison between tube in this windshield and in open).

3.1.5 Temperature gradients.

Measurement of temperatures at various positions in a cross-section of a tube solarimeter are necessary in understanding the energy balance of the solarimeter. A tube solarimeter was placed inside a windshield of 1 x 1 x 1m of polythene , tube height was 40cm. The temperature profile of the site with the windshield is shown in Fig.8. Eight thermocouples, were placed in a tube solarimeter as shown in figure 8. Temperatures of two surfaces at the center and at one end of the tube, under the glass and over the glass, air temperature and wind speed were measured. This was originally done under various environmental conditions:

i) low wind speeds and high ambient temperatures;

ii) Moderate wind speeds (prevailing at site of measurement) and normal air temperature.

3.1.6 Painting of thermocouples.

The thermocouples placed in the tube solarimeter were affected by thermal radiation load, since they were not shielded. An experiment was done to test this fact. Two thermocouples painted white and black respectively and a third unpainted thermocouple were exposed to solar

Figure 8

a) Diagram of a cross-section of a tube solarimeter showing the relative positions of thermocouples on the surface of the sensor element (black and white) and on the glass surfaces (inner and outer surfaces).

b) Diagram of a sensor element showing the alternating pattern of black and white painted sections. The black dots on the element represent thermocouple positions.

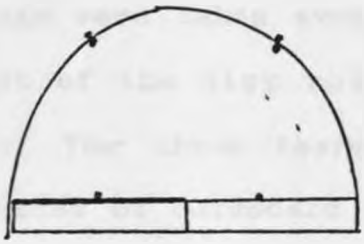

a). Cross-section

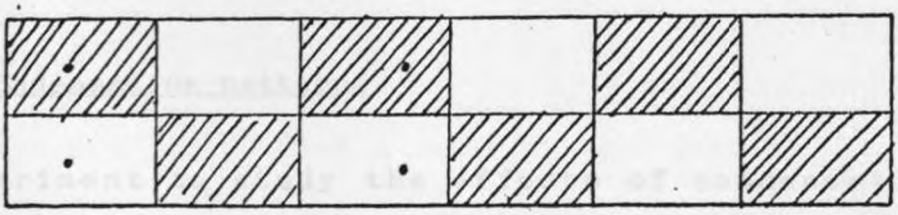

b). On the sensor element.

Figure 8

radiation. They were arranged in parallel with a spacing of 4cm between and at a height of 1m above the surface. Air temperature was measured using a shielded thermocouple. Readings were taken every five minutes for one hour. The output of the Kipp solarimeter was also taken simultaneously. The three thermocouples were then shaded (using two pieces of cardboard paper) and readings for the same duration and interval taken.

3.1.7 Temperature gradients - white painted thermocouples

Due to the effect of thermal radiation load on unpainted thermocouples, painted thermocouples were placed in a tube solarimeter and the temperature gradients measurements repeated under what appeared to be similar conditions. The thermocouple on the black painted tube solarimeter element was painted black while the rest of them were white painted.

3.1.8 Condensation patterns

An experiment to study the effects of condensation (appearance and displacement) on tube solarimeter output was done. Two tube solarimeters, one with condensation, were used. Both tubes were placed in the open with the

Kipp solarimeter as a standard. Readings were taken every 5 minutes for half an hour. Flushing of the tubes with dry air, as prescribed (using silica gel), was not tried. However, it was found that leaving a tube in dry air (not necessarily hot) without the sealing screws for some time made the condensation to disappear.

3.1.9 Placing a glass plate over tube solarimeter.

Radiation reaching a target as well as temperatures around the target, as far as depending on the radiation are modified by the introduction of a glass cover. To test the effect of change in apparent sky temperature on tube solarimeters, a glass plate of dimensions 60cm x 1m at a height of 1.25m above surface, was placed over a tube solarimeter and a Kipp solarimeter. The tube solarimeter was 1m above the ground while the Kipp was 25cm lower and the horizontal distance between them was 30cm (see figure 9). Readings were taken at intervals of five minutes for 40 minutes after which the cover was removed and recordings continued after a pause of five minutes.

Figure 9.

Photograph of experimental layout of measurement of effect of glass plate on tube and Kipp solarimeters.

Figure 9

Figure 3

3.1.10 Interfacing the Digital Thermocouple Thermometer

The Digital Thermocouple Thermometer, DTT, has ten channels which have to be read sequentially. A lot of time is lost during this process of switching and reading. To ease the data acquisition and storage an interface to the BBC microcomputer was built. The decreasing cost of microcomputers has made it possible to use them for data acquisition and experiment automation (Drake, 1987).

The DTT has a Digital Output Unit (DOU), which can be used to output digital signals from the thermometer. There are 44 pins on the DOU.

The interface was developed in two stages. The first stage involved using the BBC micro kit and sending the channel selection information from the kit. The interface kits were made available through the University of York/ODA microcomputer project. These are general purpose kits designed for teaching. They were being used here to develop an instrumentation system, since they are versatile. This was however cumbersome when serial transfer of data for long distances are needed. In the second stage this problem was overcome by using a binary counter such that all the signals required for the

Figure 10.

Timing diagrams of the interface showing the stages of multiplexer enabling and data collection. $\overline{CE1}$ - $\overline{CE4}$ are the Chip Enable signals.

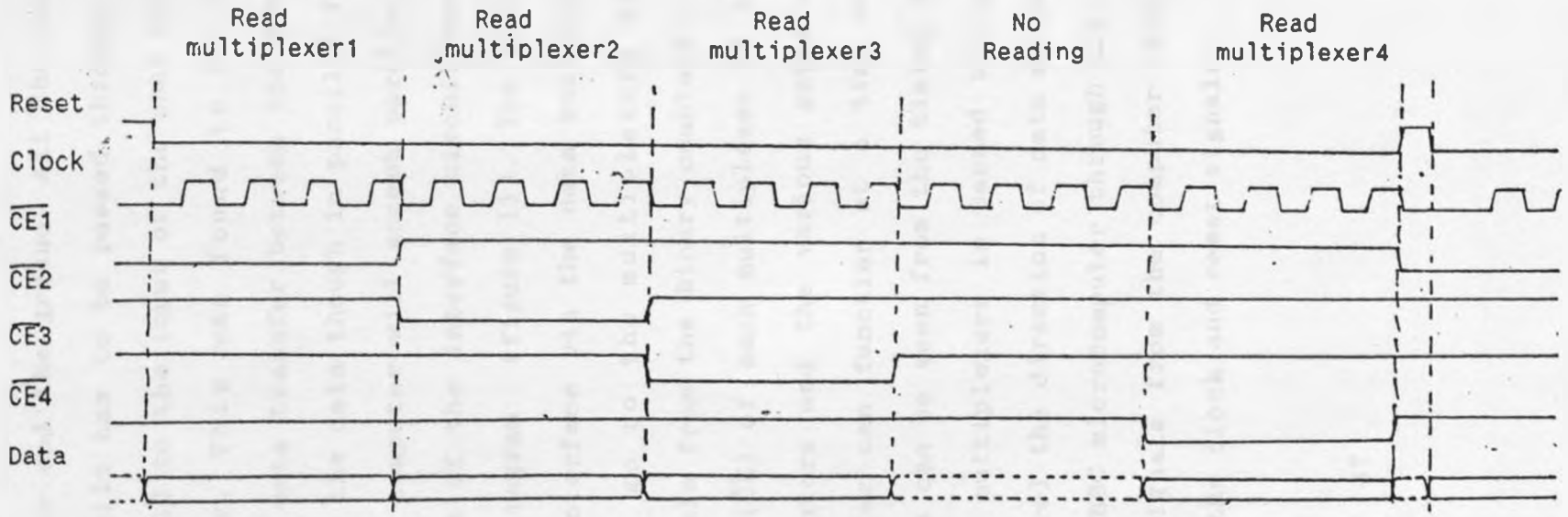
Read multiplexer1
Read multiplexer2
Read multiplexer3
No Reading
Read multiplexer4
Reset
Clock
$\overline{CE1}$
$\overline{CE2}$
$\overline{CE3}$
$\overline{CE4}$
Data

Figure 10

interface to function were three; namely the clock, the reset, the data line and the ground. All the information in the interface built has to be passed through digital multiplexers (8 to 1) to the input of the user port of the BBC microcomputer. This was found to be the most appropriate way of data transfer between the DTT and the BBC computer, since the data though in parallel format, is in BCD whereas the computer will accept parallel data in 8-bits. The details of the interface circuit can be seen in the the block diagram (figure 11). The data is made available to the interface via the data bus marked 'from DTT'. These data go to the multiplexers which are controlled by signals from the Binary counters C1 and C2. The 'chip enable' ($\overline{CE}$) of each multiplexer is controlled by the Binary counters and the various gates such that only one multiplexer can function at a time during one sampling period (as can be seen from the timing diagrams). The data from the multiplexers is passed through diodes (D1 to D4) to control the direction of data movement. This is now fed to the BBC microcomputer through the user port via a line. The signals from the computer which control the interface are the clock and reset signals.

Figure 11.

Block diagram of the interface showing the bus and line connection to various components. D1 - D4 are diodes

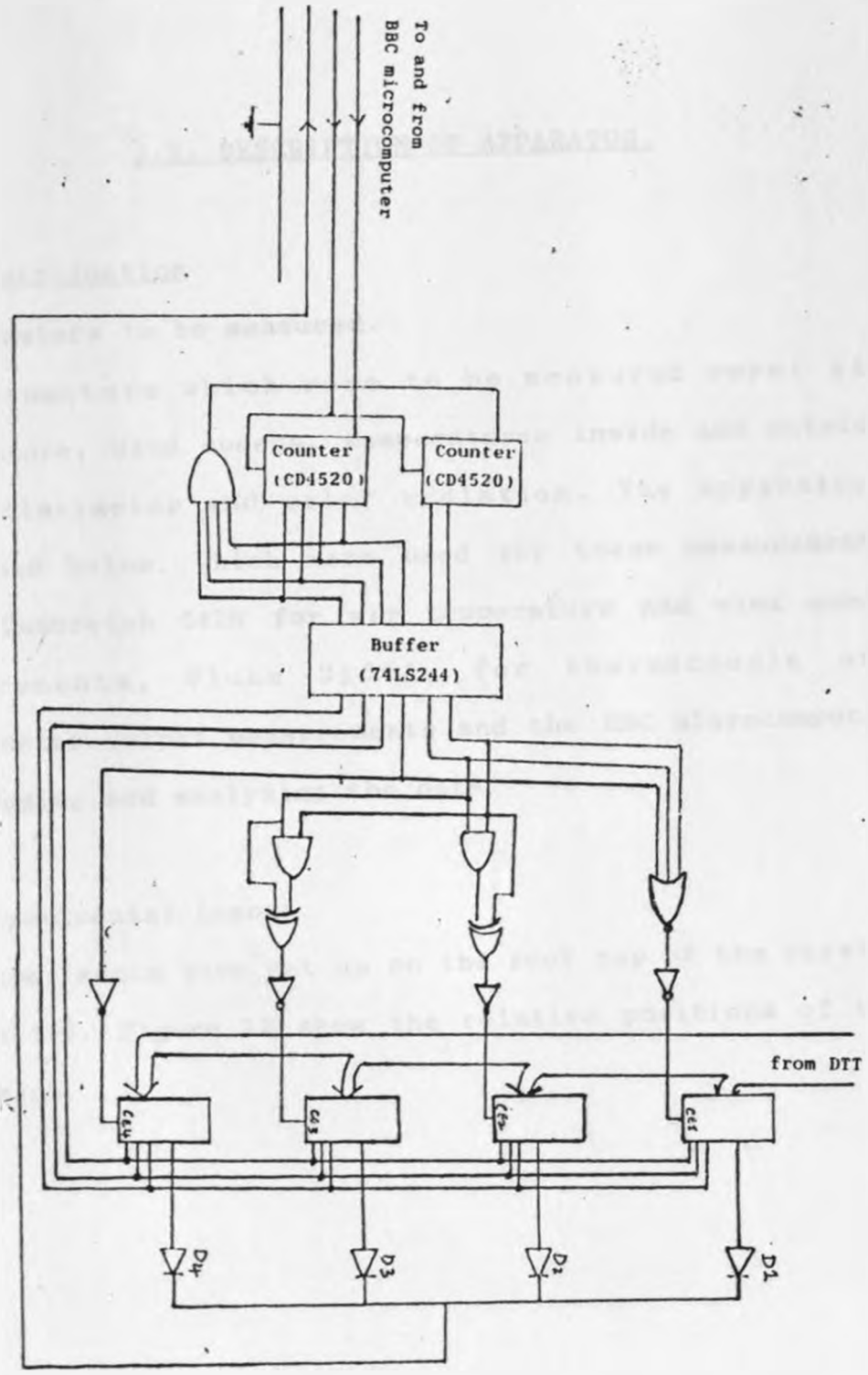
To and from
BBC microcomputer
Counter
(CD4520)
Counter
(CD4520)
Buffer
(74LS244)
from DTT
D4
D3
D2
D1

Figure 11

3.2. DESCRIPTION OF APPARATUS.

3.2.1 Introduction

i) Parameters to be measured.

The parameters which were to be measured were: air temperature, wind speeds, temperatures inside and outside tube solarimeter and solar radiation. The apparatus, described below, which were used for these measurements were; Lambretch 642N for air temperature and wind speed measurements, Fluke 2100A, for thermocouple and solarimeter output measurements and the BBC microcomputer for logging and analysing the data.

ii) Experimental Layout

The experiments were set up on the roof top of the Physics laboratory. Figure 12 show the relative positions of the apparatus.

Figure 12.

Sketch map showing the relative positions of the various apparatus to each other and to the nearby wall.

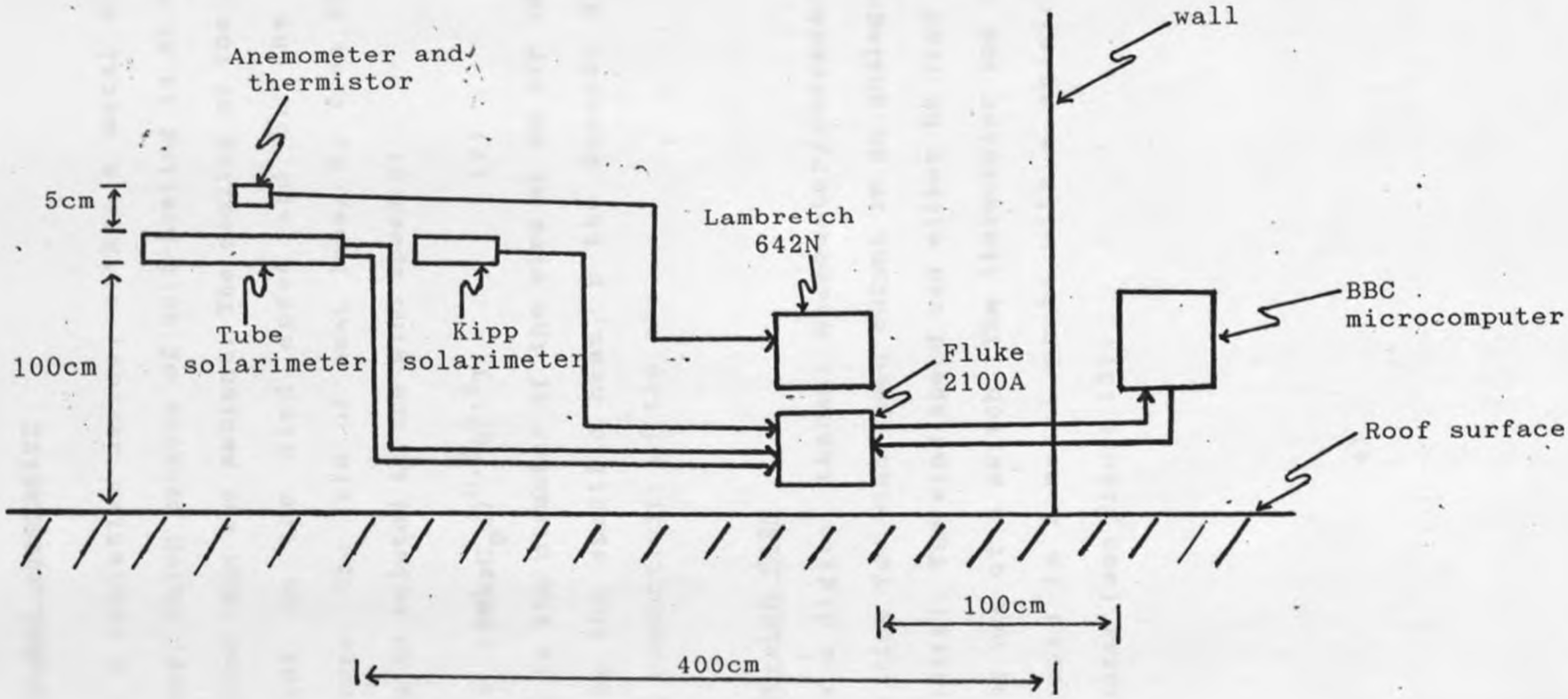
wall
Anemometer and thermistor
5cm
Lambretch 642N
BBC microcomputer
Tube solarimeter
Kipp solarimeter
100cm
Fluke 2100A
Roof surface
100cm
400cm

Figure 12

3.2.2 Thermal anemometer

This is a resistive device, either a metal wire or a thermistor, which because of self-heating is at a greater temperature than the ambient. The cooling of the sensor is dependent on the wind speed and on the ambient temperature. The rate of heat loss, H, from the heated wire can be related to the wind speed u:

$$H = kT + (2\pi k \rho C_p d)^{0.5} u^{0.5} T \qquad (7)$$

where d is the diameter of the wire at an air temperature T, C_p is the specific heat, p the density and k the thermal conductivity of the air.

(i) Lambretch 642N

This is a digital thermal anemometer/thermometer with capabilities for wind speed output in an analogue form (0 to 10 volts). The wind speed can either be read in m/s or ft./s by use of a switch. The thermometer and anemometer are housed in a metal probe with a shield for the thermometer (see figure 13).

Figure 13.

(a) Photograph of a hot wire anemometer Lambretch 642N. The rod houses the hot wire anemometer for wind speed and a thermistor for air temperature.

(b) Diagram of a constant temperature hot wire anemometer (after Woodward and Sheehy 1983). R_1, R_2 are resistors, R_D is variable resistor and R_a is a thermistor, A is an amplifier and E is output voltage.

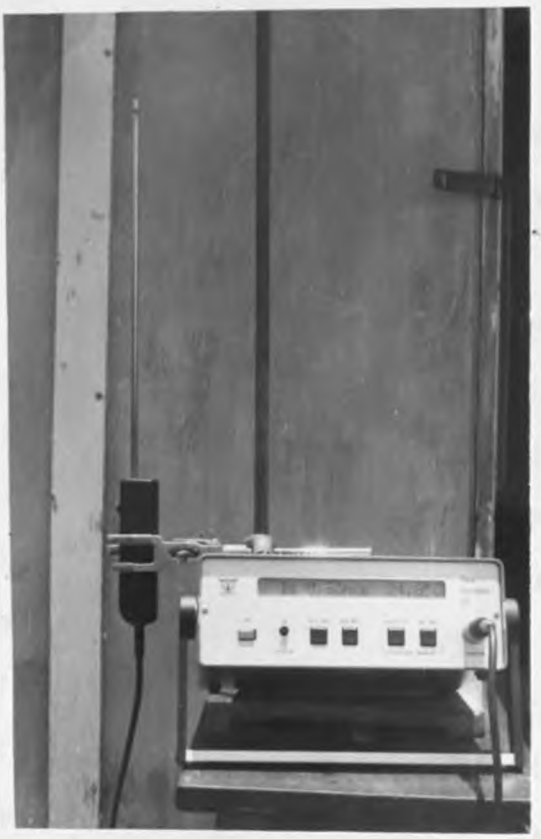

(a)

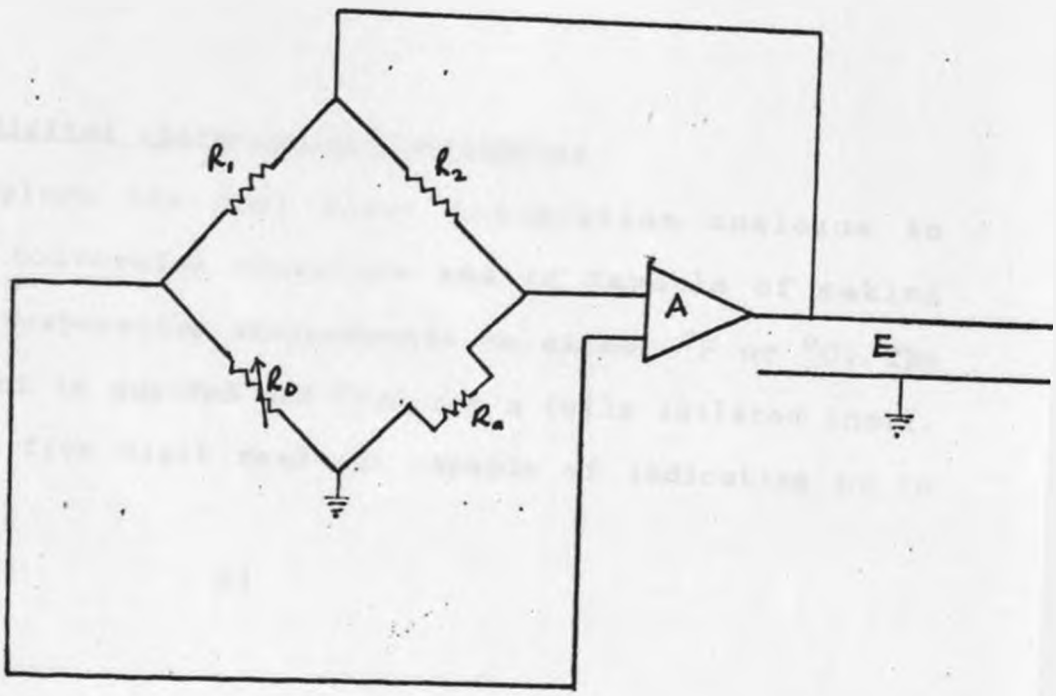

(b)

Figure 13

(ii) Design and operation

Design and operation can be seen in figure 13 (b). The design is known as a constant - temperature device. It relies on a servo amplifier ,A, to control its temperature. The output of the bridge is set at zero wind speed by R_D, so that the output is zero. (This also adjusts the variations in ambient temperature). When the device is placed in a windstream the resistance of the wire sensor R_a, will decrease by convectional cooling. The bridge then becomes unbalanced and this imbalance is fed to the amplifier as a voltage. This voltage is amplified and fed back into the bridge increasing the current through R_a and therefore increasing its temperature. Equilibrium will occur when R_a is heated so that its resistance equals R_D (i.e. original setting at zero wind speed).

3.2.3 Digital Thermocouple Thermometer

This employs the dual slope integration analogue to digital conversion technique and is capable of making precise temperature measurements in either ^{o}F or ^{o}C. The instrument is guarded and features a fully isolated input. It has a five digit read-out capable of indicating up to

Figure 14.

Block diagram of the Digital Thermocouple Thermometer (Fluke 2100A), showing the connections to the various processes.

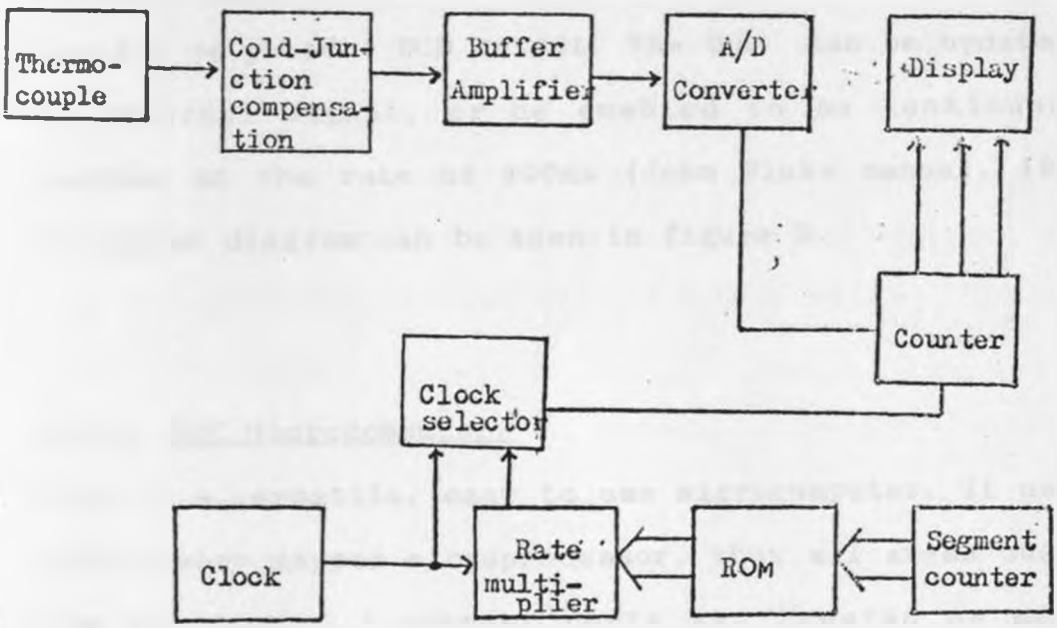
Thermo-couple
Cold-Junction compensation
Buffer Amplifier
A/D Converter
Display
Counter
Clock selector
Clock
Rate multiplier
ROM
Segment counter

Figure 14

± 3999.9 degrees. This range is however determined by the choice of the type of thermocouple in use (i.e types J,K,T,E,R and S). The resolution is to 0.1 degree. It has a multipoint switching unit capable of an input of up to ten thermocouples of the same type. It also features a Digital Output Unit (DOU) which permits the instrument to be interfaced with digital instrumentation (e.g. printer, computer etc.). The DOU has isolated parallel, 8-4-2-1 weighted , BCD output. The DOU can be updated by an external signal, or be enabled to be continuously updated at the rate of 400ms (John Fluke manual, 1975). The block diagram can be seen in figure 9.

3.2.4 BBC Microcomputer.

This is a versatile, easy to use microcomputer. It uses a 6502 memory mapped microprocessor, thus all areas such as the I/O (input / output) ports are treated as memory locations by the computer. It has BBC BASIC with an inbuilt Assembler which makes it easy to switch between BASIC and Assembler languages. It has various ports for interfacing; these are: Analogue port, User (Parallel) port, 1MHZ bus and RS423 (which is compatible to RS232)

serial port. The final interface built in this project uses the user port.

(i). The User Port.

This uses the 6522 Versatile Interface Adapter (VIA). It is in memory location between $FE60_H$ and $FE6F_H$. The 6522 VIA contains two 8-bit Input/Output ports (A and B). It has two sides i.e. the A side which is used for a parallel printer and the B side which is used as the user port.
Each pin can be individually selected to be an input or output. It has four status control lines (two for each side), two 16-bit counter timers which can be used to generate or count pulses, an 8-bit shift register which can convert data between serial and parallel forms and interrupt logic.
The operation of the chip is determined by the contents of the four registers;
1) Data Direction Register A (or B) ,DDRA (or DDRB). This determines whether the pins on port A (or B) are inputs (0s) or outputs (1s).
2) The Pheripheral Control Register (PCR). This determines the polarity of transition (rising edge or falling edge) is recognised on the input status lines (CA1 and CB1) and

Figure 15.

Diagram of the BBC microcomputer user port. PB1 - PB7 are the Port B data lines. CB1 and CB2 are the control lines and GND are the ground lines.

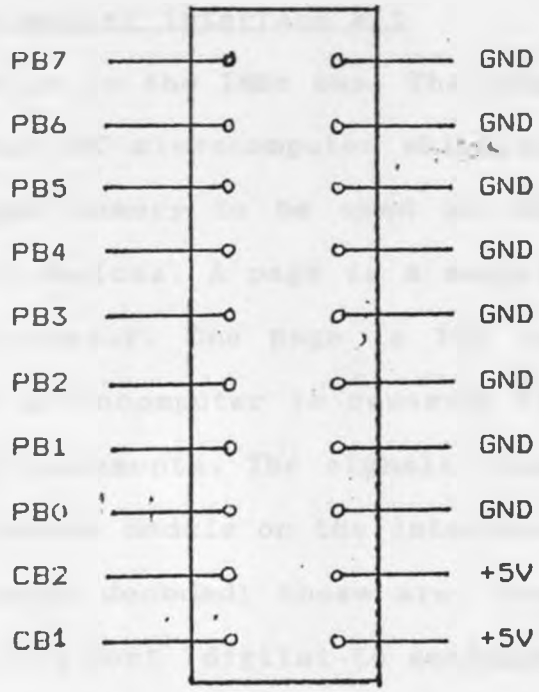
PB7
PB6
PB5
PB4
PB3
PB2
PB1
PB0
CB2
CB1
GND
GND
GND
GND
GND
GND
GND
GND
+5V
+5V

Figure 15

how the other status lines (CA2 and CB2) operate.

3) The Auxiliary Control Register (ACR). This determines whether the data ports are latched and how the timers and shift registers operate. Once the VIA has been configured, its data registers may be used like any other memory location (Bray et al, 1983).

(ii). The BBC microcomputer interface kit

The kit is connected on to the 1Mhz bus. The 1Mhz bus is an interface port on the BBC microcomputer which allows up to 64 kilobytes of paged memory to be used as well as 255 direct memory mapped devices. A page is a memory location in the 6502 microprocessor. One page is 100 bytes long. Page FC_H in the BBC microcomputer is reserved for devices with small memory requirements. The signals from this bus are decoded by the decode module on the interface kit.

The kit has three ports decoded; these are: the I/O port (input/output); the D/A port (digital to analogue) and the A/D port (analogue to digital). The decode module decodes the interface kit stating from address $FCC0_H$ to $FCC2_H$ i.e. the I/O port is decoded as $FCC0_H$; the D/A port is $FCC1_H$ and the A/D port is $FCC2_H$. The busy line is decoded as $FCC3_H$ (BBC Interface manual, 1980).

CHAPTER FOUR

4 RESULTS AND DISCUSSIONS

All experimental results reported in this chapter were preceded by a lot of trials to determine their most appropriate set-up and the order of magnitude to be expected for the parameters and phenomena reported on. Hence the data presented here are a representation of the results found in the experiments.

4.1 TEMPERATURE AND WIND SPEED GRADIENTS.

Ratios of tube to Kipp solarimeters and air temperature examples are given in figures 17 and table III. In this representative example of high radiation loads and high ambient temperatures, under conditions of low wind speeds the output of the tube solarimeter relative to a Kipp solarimeter increased by between 8% and 17%, with an average of 12%.

In an earlier experiment of this kind, under even more extreme conditions of very low wind speeds (0.31 m/s) and tube height of 40cm from surface, the differences in the TSL/Kipp ratio went up to 55% with an average of 48%. Part of this high value was due to differences in time constants between the two instruments since readings were taken every minute.

The ratio of tube to Kipp solarimeter in the windshield shows an increase with time even though there is no appreciable increase in air temperature (Fig. 17a). This increase can be attributed to low wind speeds in the windshield which lead to low rates of heat removal form the tube solarimeter.

Table III

Comparison of air temperatures, wind speeds and ratios of tube to Kipp solarimeters in open air and inside windshield. Wind1, air1 and ratio1 refer to wind speeds, air temperature and ratio TSL/Kipp in the open. Wind2, air2 and ratio2 refer to same measurements inside windshield.

Time (mins)	wind1 (m/s)	air1 (^{o}C)	wind2 (m/s)	air2 (^{o}C)	ratio1	ratio2
0	0.20	37.9	0.52	36.2	2.063	1.906
5	0.28	40.0	2.20	33.7	2.093	1.911
10	0.39	39.6	2.20	32.4	2.096	1.899
15	0.20	38.9	0.35	33.8	2.112	1.910
20	0.20	38.5	3.80	32.0	2.106	1.764
25	0.18	40.1	1.13	31.1	2.112	1.915
30	0.04	40.2	0.98	32.8	2.176	1.982
35	0.19	39.5	2.10	32.1	2.195	1.970
40	0.29	39.0	0.22	32.8	2.202	1.880
45	0.19	39.5	1.16	31.2	2.201	1.890

In the open however, variations in output can be seen (figure 16a). The fall in ratio for measurement at 20 mins was caused by a cloud cover occurring about 15mins after

Figure 16.

a) Graph of Tube solarimeter output to Kipp solarimeter output ratio in the open (—+—) and inside the windshield (—□—).

b) Graph of air temperature within windshield (—□—) and in the open (—+—), taken simultaneously with TSL/Kipp ratios (Graph a).

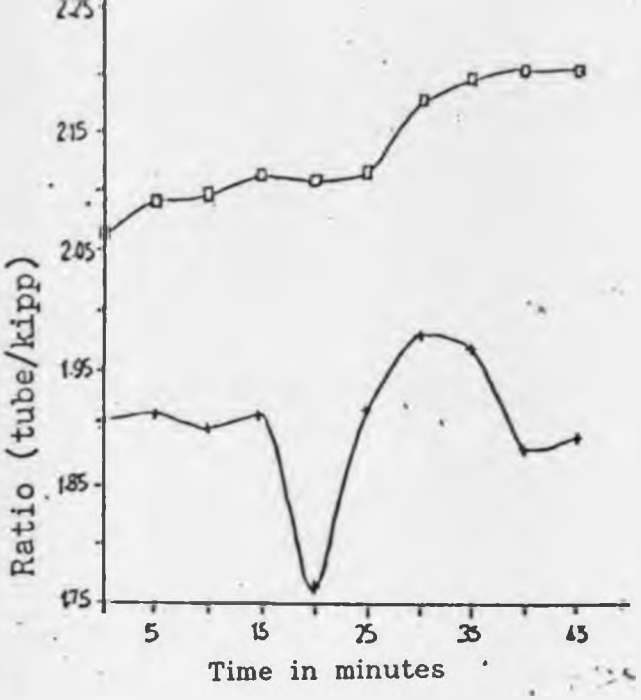
Ratio (tube/kipp)
2.15
2.05
1.95
1.85
1.75
5
15
25
35
45
Time in minutes

(a)

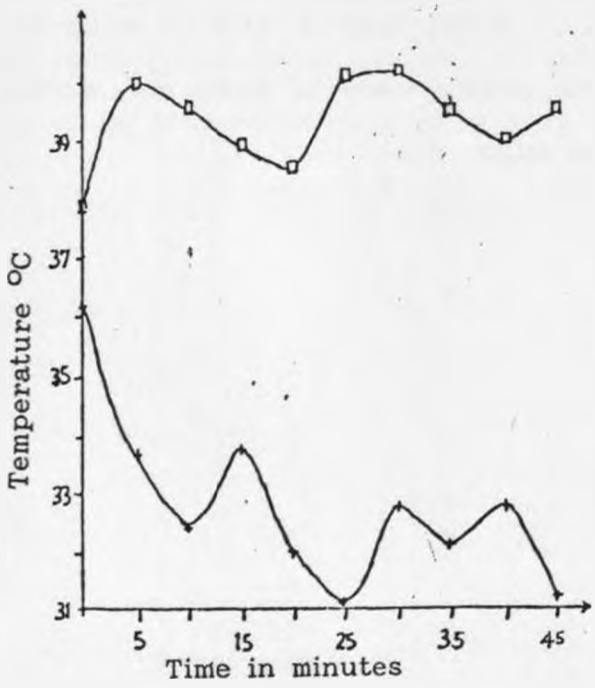
Temperature °C
39
37
35
33
31
5
15
25
35
45
Time in minutes

(b)

Figure 16

Figure 16

c) Graph of wind speeds within windshield (—+—) and in the open (—x—). Data was measured using a Lambretch 642N.

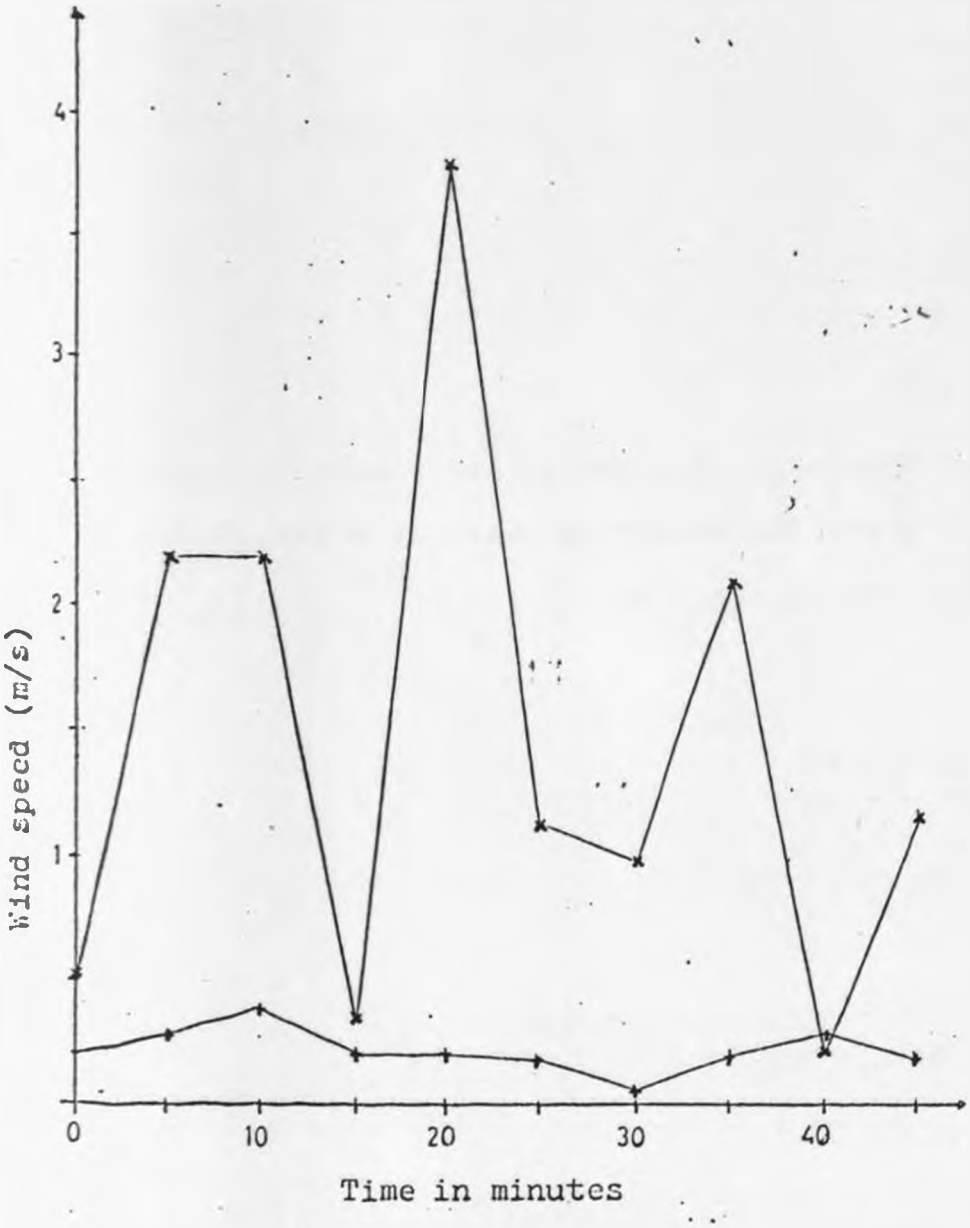

Figure 16 (c)

Figure 17.

Graph of TSL/Kipp solarimeters ratio over a period of five hours. The Kipp/Kipp ratio is a horizontal straight line on the graph.

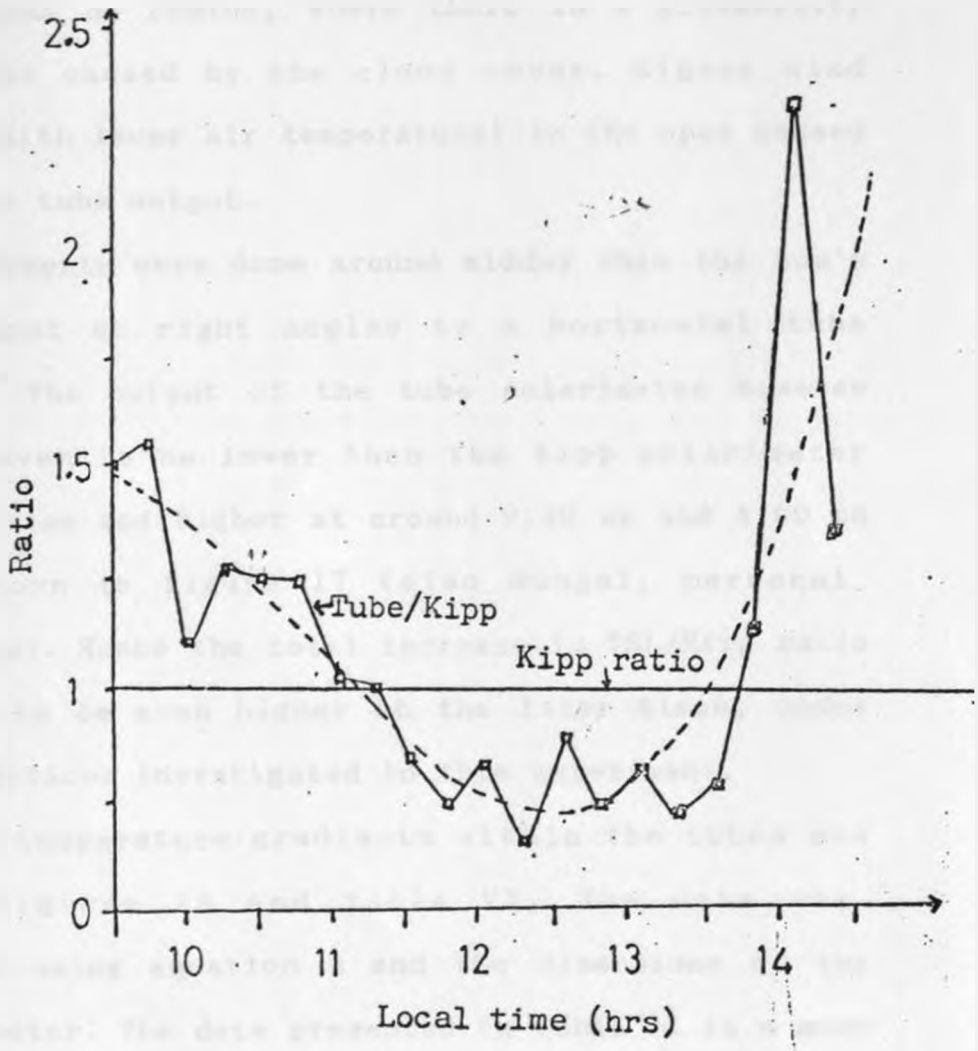
2.5
2
1.5
1
0
Ratio
Tube/Kipp
Kipp ratio
10
11
12
13
14
Local time (hrs)

Figure 17

start of the experiment and lasting for about 30 seconds. As the tube recovers, the output goes higher than before until it stabilizes later. Wind speed did not show much variation, (Figure 16c) however the random variations in air temperature may have been caused by wind speeds except for measurement at 25mins, where there is a probability that this was caused by the cloud cover. Higher wind speeds and (with lower air temperature) in the open caused a drop in the tube output.

These measurements were done around midday when the sun's beam is almost at right angles to a horizontal tube solarimeter. The output of the tube solarimeter however has been proven to be lower than the Kipp solarimeter around this time and higher at around 9.00 am and 4.00 pm which is shown in figure 17 (also Mungai, personal communication). Hence the total increase in TSL/Kipp ratio is expected to be even higher at the later times, under similar conditions investigated in this experiment.

Examples of temperature gradients within the tubes are shown in figures 18 and table VI. The data was interpolated using equation 3 and the dimensions of the tube solarimeter. The data presented in table VI is a mean of ten readings. Within the windshield (high ambient

Figure 18.

Graphs of temperature patterns in a radial cross-section of tube solarimeter. Distance 0cm is on the sensor plate, 1.5cm is on the inner side of glass surface, 1.65cm is on the outer glass surface. The smooth curve joining the data points was obtained by use of equation 3. (—+—) is on white side and (—o—) is on black side.

a) Data taken inside a windshield (high ambient temperature).

b) Data taken in the open under diffuse radiation.

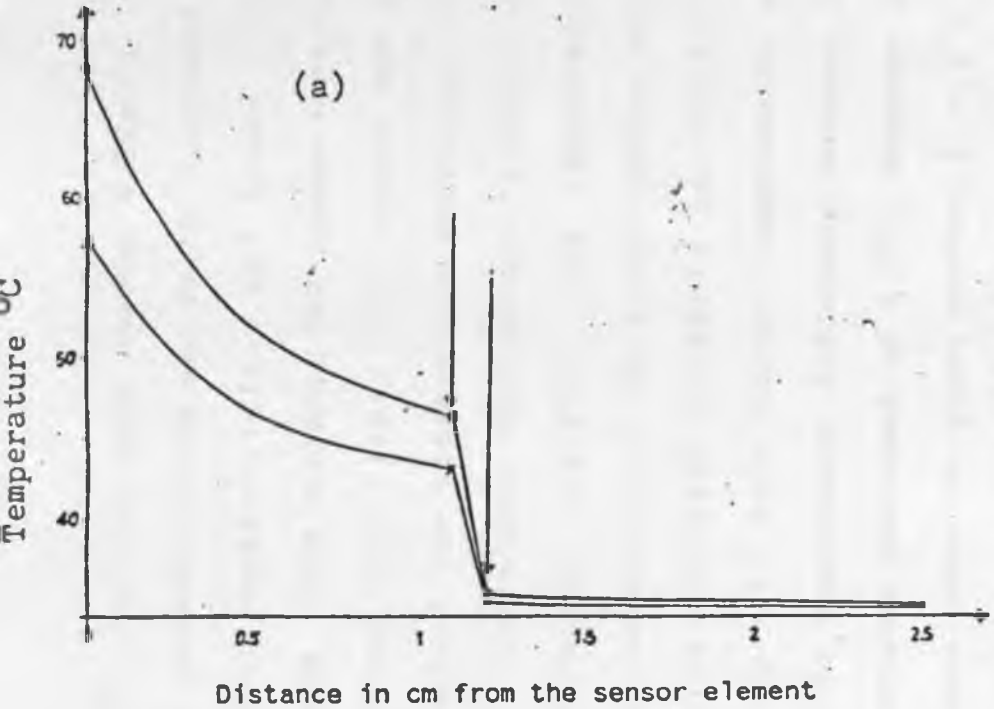
(a)
Temperature °C
70
60
50
40
0.5
1
1.5
2
2.5
Distance in cm from the sensor element

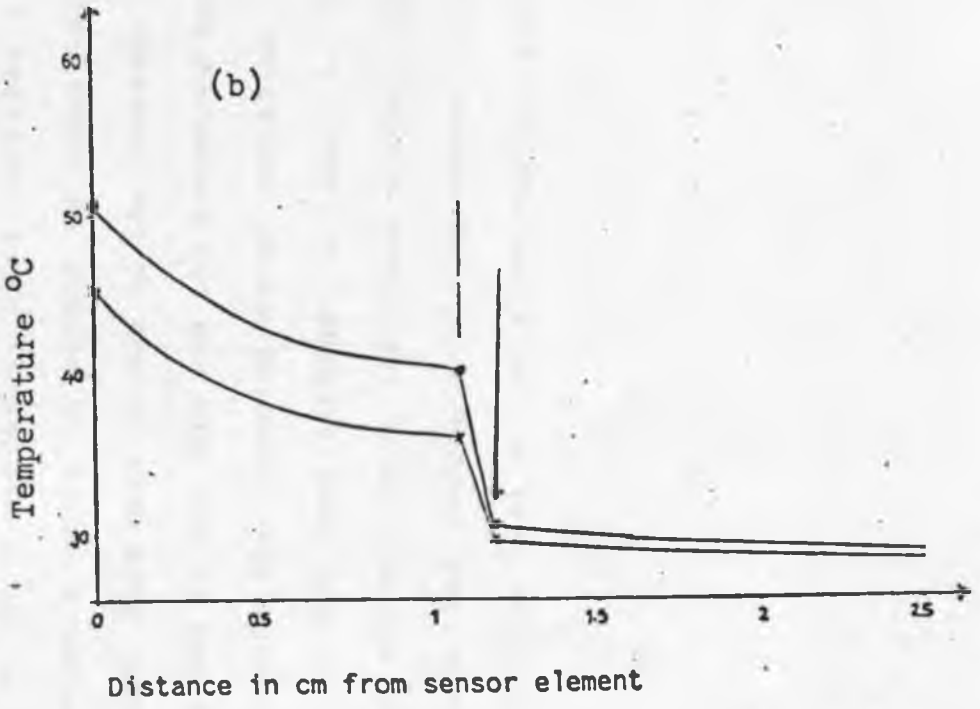
(b)
Temperature °C
60
50
40
30
0
0.5
1
1.5
2
2.5
Distance in cm from sensor element

Figure 18

temperatures ,39.3°C, and low wind speeds, 0.22m/s), the temperature of the surfaces (black and white) increased by 17.7°C and 12.3°C respectively, and hence their differences increased. This explains the higher tube/Kipp ratios under identical conditions. Wind speeds and air temperature also affect the temperature gradients of a tube solarimeter. With higher wind speeds (1.47m/s) and lower air temperatures (32.8°C), the temperature differential on the underside of the glass surface above the black and white surfaces slightly increased as compared to the case with high ambient temperatures and low wind speeds. The temperature difference between the black and white surfaces decreased to 5.5°C. However the temperature difference under the glass surface is 4.2°C as compared to 3.4°C in the windshield. This confirms the fact that the tube as a whole is warmed up appreciably above air temperature. This must be due to the increase in the heat energy trapped in the tube and the decreased heat exchange, combined with the incoming solar radiation in the latter case. [As this heat exchange is lower, in the case (a), the glass surface above the black surface gets warmer but the convection currents rising above this surface take part of this heat to the glass surface above

the white surface and down the white surface. The fact that the wind reached the tube part over the measured white surface first may have contributed to the cooling.] This can be seen from the smaller temperature difference at the glass surface above the black and white surface as compared to the case in the open. It should be observed that under all conditions the white surface is also heated appreciably above the temperature that might be expected from its absorption alone (since it is a reference surface of the solarimeter). This shows the importance of the convection phenomena within the tube, bringing part of the heat from the black surface over to the white surface. [It may be speculated upon that the outer surface temperatures are closer to air temperature in the case (a) (Table IV) due to high long wave radiation exchange with the clear sky compared to case (b), where low ambient temperature may have reduced such an exchange]. Convection currents along the tube also exists as evidenced by the differences in temperatures of the surfaces between the center and one end of the tube. The outer ends are cooler and this effect is larger on the black surface with an average of 3.75^{o}C (maximum 8.6^{o}C) as compared to 1.7^{o}C (Maximum 5.5^{o}C) for white surface. These two convection

Figure 19.

Diagrams showing the possible convection patterns in a tube solarimeter. The arrows show possible direction of air flow.

a) Cross-section of a tube solarimeter. Convection between the black and white surface in a cross-sectional part of a tube solarimeter.

b) Between adjacent black and white surfaces along the tube solarimeter.

c) Between the center and the ends of a tube solarimeter.

(a)

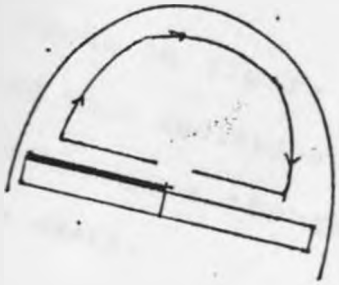

(b)

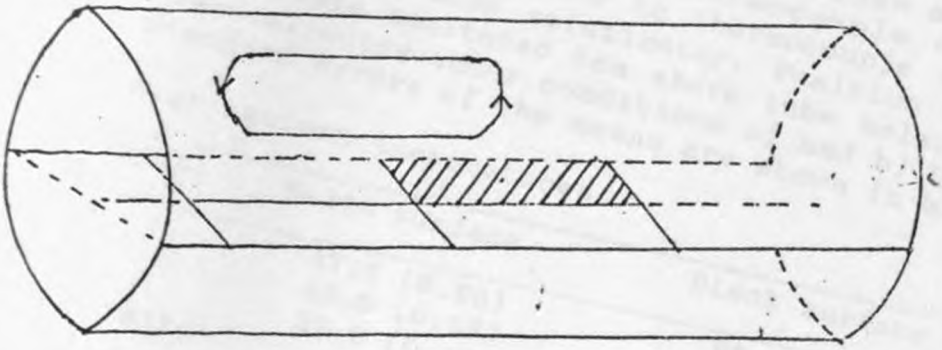

(c)

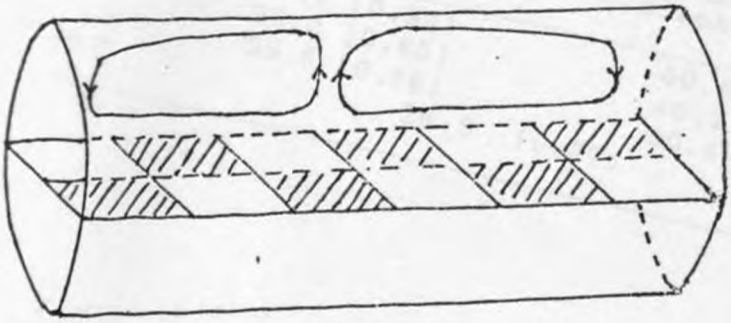

Figure 19

patterns are shown in figure 19 . Under high ambient temperatures and high radiation loads, the temperature of the surfaces were higher though the increase in their differences were small.

Table IV

Comparison of cross-sectional temperatures in a tube solarimeter. The positions of thermocouples are 0 - on the sensor element, 1 refers to thermocouple on the inner glass surface and 2 refers to thermocouple on the outer glass surface of tube solarimeter. Position 3 refers to air temperature monitored 5cm above tube solarimeter. The data was collected under conditions a) and b) below. The standard errors of the means are shown in brackets.

(a) High ambient temperatures.

Position	White surface	Black surface
0	57.4 (0.90)	68.3 (0.63)
1	43.0 (0.69)	46.4 (0.67)
2	35.0 (0.42)	35.4 (0.36)
3 (air)	34.1 (0.51)	

(b) Low ambient temperatures.

Position	White surface	Black surface
0	45.1 (0.99)	50.6 (0.62)
1	36.0 (0.65)	40.2 (0.87)
2	29.5 (0.56)	30.4 (0.52)
3 air	26.8 (0.37)	

It may again be concluded that the increase in tube solarimeter to Kipp solarimeter ratios is due to the combined effect of high ambient temperatures and low wind speeds.

4.2 PAINTING OF THERMOCOUPLES.

Thermocouples painted black showed a similar response to solar radiation as a Kipp solarimeter. However, a white painted thermocouple behaved very much like a shaded thermocouple. On the other hand, an unpainted thermocouple followed the trend of a black painted thermocouple, though the amplitude was smaller. When all the thermocouples were shaded, the picture was different with all the thermocouples showing the same trend, i.e. showing air temperature. The results are presented in table V below and figure 20. The thermocouples were arranged parallel to the wind direction. Sky conditions were generally clear except for a brief period of cloud as can be seen from figure 20.

Table V

Comparison of painted and unpainted (bare) thermocouples under two conditions a) and b) below.
All data taken at an interval of 5 minutes.

(a) Thermocouples exposed to solar radiation

White (°C)	bare (°C)	black (°C)	air (°C)	Kipp (mV)	wind (m/s)
27.1	30.8	33.1	27.0	10.866	0.11
27.6	31.4	32.5	27.2	9.882	0.04
27.9	31.2	32.1	27.0	10.115	1.10
28.1	31.0	33.5	28.6	10.941	1.40
28.7	31.6	33.8	29.1	11.211	1.03
28.6	31.3	33.9	28.5	10.521	1.76
27.0	30.6	33.3	26.1	8.866	0.89
27.3	29.9	33.4	27.8	9.218	0.54
27.0	30.1	33.6	27.2	9.675	0.33
27.8	29.7	32.8	28.1	10.110	0.07
27.9	29.8	32.5	28.0	10.205	0.14
28.0	30.3	32.9	27.9	10.128	0.02

(b) Shaded thermocouples.

white (°C)	bare (°C)	black (°C)	wind (m/s)
26.9	26.2	27.2	0.06
27.2	27.9	27.6	0.19
26.0	25.5	26.2	0.82
26.5	26.7	26.5	1.02
26.7	25.2	25.9	1.95
27.5	28.2	28.8	0.77
25.8	26.8	26.1	2.01
26.1	27.1	27.0	1.56
24.8	25.0	25.8	1.78
23.5	24.2	24.3	2.50
26.2	25.1	25.9	2.11
26.5	26.6	26.0	1.07

Figure 20

Graphs of outputs of painted and unpainted thermocouples under two radiation conditions.

a) Direct radiation (unshaded thermocouples). Air temperature measured by painted and unpainted thermocouples are: Δ——Δ is black painted thermocouple, □——□ unpainted thermocouple, +——+ air temperature (measured by Lambretch 642N), o——o white painted thermocouple and x——x is output of Kipp solarimeter.

b) Shaded thermocouples. Δ——Δ black painted, □——□ unpainted, and o——o white painted thermocouples.

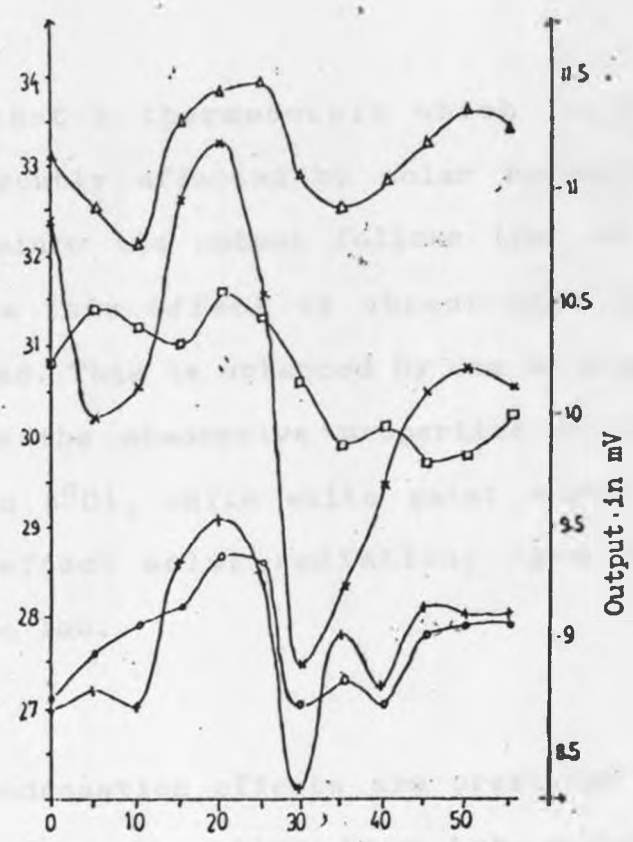

a) unshaded

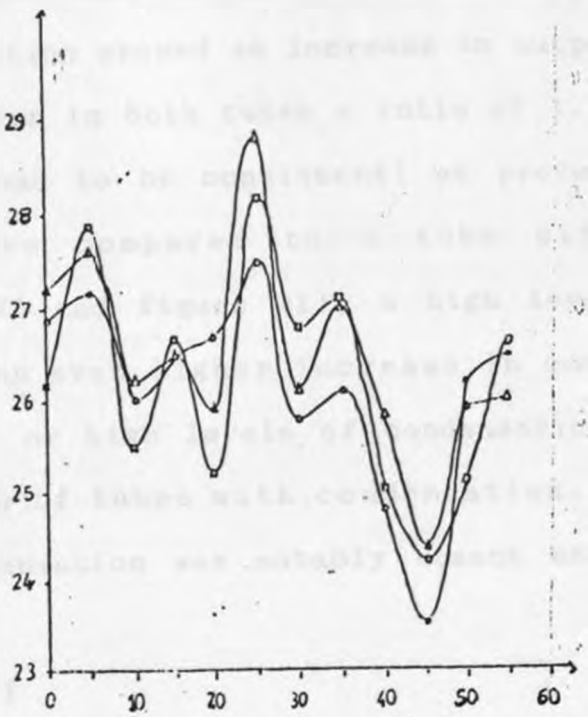

b) shaded

Figure 20

It may be concluded that a thermocouple which is not painted white is apparently affected by solar radiation load when un-shaded, since its output follows that of a Kipp solarimeter while this effect is absent when the thermocouples are shaded. This is enhanced by use of black paint, which increases the absorptive properties of the thermocouple (by up to $6^{o}C$), while white paint virtually provides a shading effect solar radiation, when the wind speeds are not too low.

4.3 CONDENSATION.

The results on the condensation effects are presented in tables VI. Presence of condensation in a tube gave a reading which was higher than in its absence. A tube with low levels of condensation showed an increase in output of 4% [with no condensation in both tubes a ratio of 1.13 of tube2 : tube1 was found to be consistent] at prevailing ambient temperatures compared to a tube without condensation (table VI and figure 21), a high level of condensation showed an even higher increase in output. Distinguishing of low or high levels of condensation was by visual comparisons of tubes with condensation. This increase due to condensation was notably absent at very

high ambient temperatures.

Table VI

Comparison of cross-sectional temperatures in a tube solarimeter. The positions of thermocouples are 0 - on the sensor element, 1 refers to thermocouple on the inner glass surface and 2 refers to thermocouple on the outer glass surface of tube solarimeter. Position 3 refers to air temperature monitored 5cm above tube solarimeter. The data was collected under conditions a) and b) below.
The standard errors of the means are shown in brackets.

(a) Sunny conditions, tube solarimeter with condensation.

Position	White surface	Black surface.
0	51.9 (0.42)	61.9 (0.32)
1	38.9 (0.27)	45.4 (0.42)
2	34.6 (0.32)	37.0 (0.28)
3 (air)	31.8 (0.27)	

(b) Diffuse conditions

Position	white surface	black surface
0	43.3 (0.44)	55.4 (0.55)
1	33.5 (0.36)	44.3 (0.51)
2	30.4 (0.39)	33.6 (0.23)
3 (air)	28.5 (0.11)	

(c) Outputs (mV) of two tube solarimeters and a Kipp solarimeter sunny conditions. Tube1 had condensation while Tube2 had no condensation. Average wind speed (m/s) during the measurement period is also given.

Tube1	Kipp	Tube2	Wind
25.536	13.348	27.741	1.37
(0.191)	(0.145)	(0.169)	(0.16)

Table VI

(d) Outputs (mV) of two tube solarimeters and a Kipp solarimeter diffuse conditions. Tube1 had condensation while Tube2 had no condensation.

Tube1	Kipp	Tube2	Wind
15.610	9.499	17.487	0.85
(0.155)	(0.174)	(0.153)	(0.11)

This is in line with observations of condensation at cooler ends of the tube under other ambient conditions. This increase in percentage therefore also depended on the amount of solar radiation falling on the tube. When put out in the sun, condensation starts over the black surface and lateral movement over to the white surface is observed after some time. This suggests that convection currents that pass under the glass above the black surface has to do with the onset of condensation. Orientation played an important role in the spread of condensation in the tube solarimeter. In the N/S orientation, the condensation, which always was mostly over the white surfaces, was heavy on the eastern facing side of the solarimeter which later in the day (around 9.00am) spread evenly over to the other white sides. The opposite trend was seen in the evening.

Figure 21.

Graphs of temperature patterns in a radial cross-section of tube solarimeter. Distance 0cm is on the sensor plate, 1.5cm is on the inner side of glass surface, 1.65cm is on the outer glass surface. The smooth curve joining the data points was obtained by use of equation 5. (—+—) is on white side and (—o—) is on black side.

a) Under sunny conditions in the open and with no condensation in tube solarimeter.

b) Under sunny conditions , tube solarimeter having condensation.

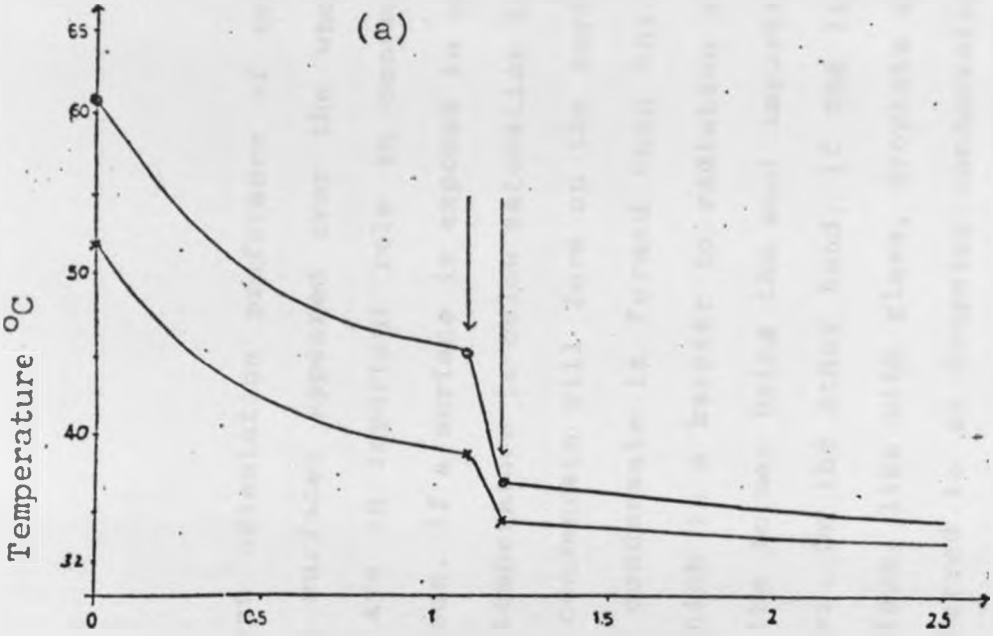
(a)
65
60
50
40
32
Temperature °C
0
0.5
1
1.5
2
2.5
Distance in cm from the sensor element

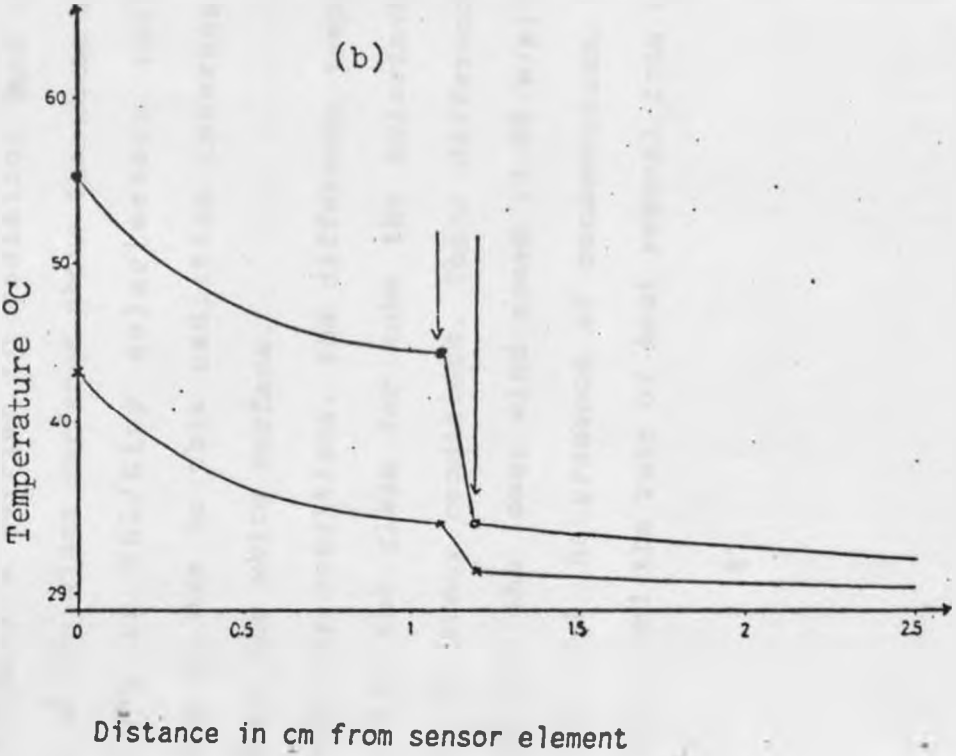
(b)
60
50
40
29
Temperature °C
0
0.5
1
1.5
2
2.5
Distance in cm from sensor element

In the East/West orientation preference of condensation over the white surfaces appeared over the whole tube . Condensation plays an important role in convective heat transfer processes. If a surface is exposed to condensable vapour and its temperature is below saturation temperature of the vapour, condensate will form on the surface. If a smooth film of condensate is formed then this is film condensation, which is a barrier to radiation as well as heat exchange, the former being the most important in non - opaque surfaces. On the other hand, if the liquid does not wet the surface, like with glass, droplets are formed and this is referred to as dropwise condensation, which again is largely a barrier to radiation and occurred preferably at the glass surfaces above the white surfaces. The increase in TSL/Kipp solarimeters ratio with condensation is due to this radiation interception by droplets above the white surface.

Under diffuse sky conditions, the difference temperatures under and over the glass for tube the solarimeter were larger than in sunny conditions. These differences were brought about by the lower wind speed (0.85 m/s) passing over the tube and the presence of condensation. Low air movement suppressed the rate of heat removal from the tube

the solarimeter. On the other hand, presence of condensation over the white surfaces kept the glass surfaces cooler hence the larger differences (compare Tables IV and VI).

4.4 PLACING OF GLASS PLATE OVER TUBE SOLARIMETER

A glass cover placed over a tube solarimeter and a Kipp solarimeter gave 17% and 8.7% reduction in output as compared to no glass cover used with the same instruments (table VII). No explanation can be found for the higher tube/Kipp ratios in the open other than from pure radiation sources. If the pyrex used by Delta-T Devices in the tube solarimeter and the glass used by the Kipp would have the same wavelength transmission curve, placing the glass should not make a difference in reduction. But the pyrex of the tube might well be different in this respect (the data were not available), which might have caused the difference in reduction. However, the difference is most likely due to the difference in distance between glass plate and tube compared to that between the much lower placed kipp and glass plate. Under the rather hazy cloud conditions, which can be seen from figure 22, the diffuse radiation towards the Kipp was reduced appreciably by

smaller amounts. This was enhanced by the experiment being close to a wall of concrete and by other sources of diffusively reflected radiation around the experimental site. Any effect of a difference in apparent sky temperature may therefore only be found by studying the temperatures within and over the tube (see figure 22). All temperatures inside the tube indicate an increase, compared to the situation with no glass plate cover, showing that the difference in effective "sky" radiation reaching the sensing surfaces of the tube was the overwhelming factor. Considerable reduction of surface temperatures in the tube early during the start of the experiment with the glass cover do not invoke an immediate decrease of the other temperatures but only after 10 minutes. Both the outer and inner glass surface react immediately to the higher effective sky temperature with an increase. The dynamics of the temperatures after the glass removal (which were higher: white surface 0.9^{o}C and black surface 2.5^{o}C than with the glass cover) show the same trend. This interpretation means that placing a tube lower in the canopy would not only lead to reduced radiation loads but also to a counteracting effect due to the increase in effective "sky" temperature.

Table VII

(a) Outputs of tube and Kipp solarimeters (mV) under glass cover and in the open. Kipp1 and tube1 refer to outputs of Kipp and tube solarimeters respectively under glass plate cover while Kipp2 and tube2 refer to the same measurements in the open.

Kipp1	tube1	Kipp2	tube2
10.982	19.512	11.645	19.189
11.015	18.531	11.898	21.139
10.701	18.011	11.600	21.468
11.105	18.401	12.209	22.481
12.280	19.901	13.281	23.911
11.753	18.246	12.650	22.810
11.162	19.114	12.379	22.336

(b) Ratios of tube to Kipp solarimeter, these are mean figures.

In open	Under glass
1.783	1.659
(0.023)	(0.025)

(c) Temperatures (^{o}C) of various positions in tube solarimeter under conditions i) and ii) below.
bs - Black surface temperature; ws - White surface temperature; bs1 - inner glass surface temperature, above the black surface; ws1 - inner glass surface temperature, above the white surface; bs2 - outer glass surface temperature, above the black surface; ws2 - outer glass surface temperature, above the white surface and air is air temperature measured 5cm above tube solarimeter.

i) With glass cover

ws	bs	ws1	bs1	ws2	bs2	air
52.6	60.1	41.9	42.7	38.8	39.1	28.1
50.7	59.1	42.8	43.3	37.1	39.9	28.5
48.8	53.6	40.7	42.6	39.4	41.2	27.6
46.9	50.8	38.4	40.3	36.4	37.9	28.9
45.7	54.6	37.8	40.7	36.6	37.4	29.2
48.2	56.3	39.3	43.6	38.1	39.4	27.8
48.1	57.4	38.6	40.1	37.2	38.9	27.3
48.9	59.2	39.3	42.1	36.2	39.4	28.2

ii) With no glass cover

ws	bs	ws1	bs1	ws2	bs2	air
46.5	58.0	38.4	42.5	36.6	40.0	26.1
50.8	62.9	43.8	45.2	37.1	42.0	27.2
53.0	62.0	42.3	45.1	40.1	41.0	27.6
53.1	62.0	41.4	43.7	38.1	40.9	28.1
50.6	60.2	42.6	44.5	41.1	42.2	26.6
45.2	55.3	37.6	38.8	35.9	36.8	27.9
50.3	60.4	41.5	42.7	39.4	39.6	26.4
47.3	58.0	39.0	41.1	38.8	40.1	27.0

Figure 22.

Graphs of temperature patterns in a tube solarimeter under two conditions:

a) Under normal conditions and

b) Tube and Kipp solarimeters under a glass plate cover.

•——• on the sensor element, black surface

▾——▾ on the sensor element, white surface

▵——▵ on the inner glass surface, over black surface

▫——▫ on the inner glass surface , over white surface

+——+ on the outer glass surface, over black surface

x——x on the outer glass surface, over white surface

o——o air temperature measured 5cm above tube solarimeter.

Temperature in °C
25
30
40
50
60
65
0
10
20
30
Time in minutes
(a)

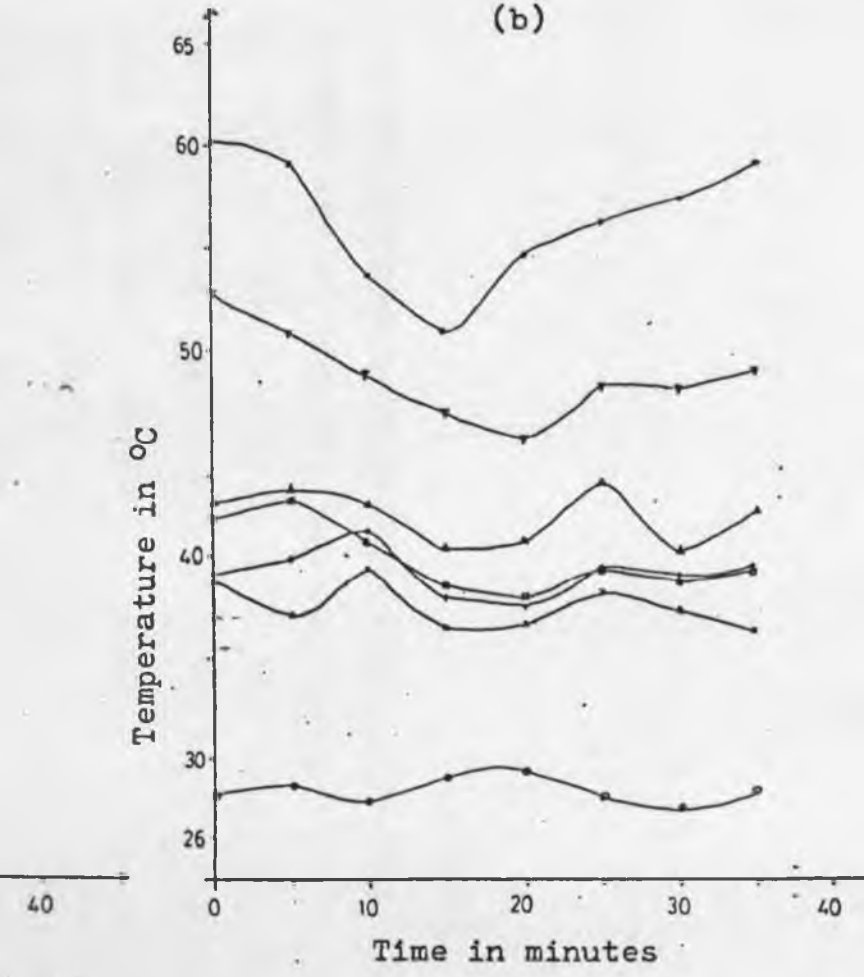

Figure 22

4.5 INTERFACING.

The DTT was interfaced to the BBC microcomputer for ease and convenience in data acquisition and analysis. The data was stored in a disk during the acquisition and later analysis was done using INSTAT a statistical package for the BBC microcomputer. This was facilitated by software written for the transfer of data between the BBC microcomputer and a data logger (Pit and Coulson, 1987). This was modified to suit the problem to be solved. software to input data from the BBC interface kit to the computer, then later to floppy disk for storage was also used (Ng'etich, 1987). Serial data transfer in the project was achieved for a 3m length of ordinary cable wire. There was no distortion in the data even though the wire was not screened. However for longer distances, it may be necessary to use screened wire. Boosting of the signals may be necessary as there is appreciable degradation over longer distances.

CHAPTER FIVE

5. CONCLUSIONS

5.1 GENERAL.

An attempt has been made to investigate energy balance trends of a tube solarimeter. The results presented in various figures and tables above proves that the solarimeter tube in its present form gives errors in its use. The outputs of tube solarimeters as such should be taken with caution if different ambient conditions of temperature, wind speed and "sky" radiation temperature are to be compared. Particularly emphasis should be laid on temperature and wind speed profiles above and within crops where these tubes are used. Condensation effects should also be taken into account. Radiation geometry effects add considerably to these errors (also Mungai et al., unpublished). The total picture of the errors has recently been reviewed (Stigter et al., 1989a; 1989b).

5.1.1 Condensation

Due to fluctuations in tropical temperatures, condensation is introduced into a tube solarimeter by contraction and expansion of the tube solarimeter seals. It preferably appears above cooler white surfaces. As shown above, such

condensation increased the tube output relative to a Kipp solarimeter, especially at higher levels of condensation. This can lead to a larger error when considered in combination with high humidity, relatively high ambient temperatures and low wind speeds. Flushing of tube solarimeters with dry air removes the condensation problem only temporarily.

Orientation also plays an important role in the spreading of condensation over the white surfaces. East/West tube solarimeter orientation showed an early spread of condensation all over the glass area above the white surfaces in the morning hours. In the North/South orientation however, condensation in the morning starts above the white surfaces on the eastern facing side of the tube, then spreads over to the western side. This changes at around 9.00 a.m., after which the condensation in the two orientations show similar patterns. The different patterns in condensation due to orientation implies different heating patterns. This is confirmed by occurring preference of condensation to the cooler outer ends of tubes under certain ambient conditions.

5.1.2 Height of tube solarimeter above surface

Studies of solar radiation penetration in a canopy makes use of tube solarimeters in at least two positions: above and below the canopy. A tube solarimeter sited below a canopy may be at the top or closer to the soil surface. The influence of the ambient temperature and emission of long-wave radiation by the crop and soil and lower air movements will then determine the performance of the tube solarimeter. The experiments with a glass plate indirectly confirm the influence of effective sky temperature, although this effect could not be quantified with this set-up.

5.1.3 Ambient temperature and wind speed

Tube solarimeters sited near warmer surfaces might experience higher ambient temperatures and lower wind speeds than those placed higher. The increase in ambient temperature at low wind speeds means lower overall cooling rates and hence a very different build-up of heat energy in a tube solarimeter. An increase in tube solarimeter to Kipp solarimeter ratios is clearly caused by this effect. At relatively low ambient temperatures, wind speed showed a weaker effect on tube output. However, at high ambient temperatures wind speed did have an

appreciable effect on the output ratio.

A glass cover over a tube solarimeter cuts the radiation reaching the tube. The output of the tube solarimeter reduced by 17%, whereas a Kipp solarimeter reduced by 8.7% under the same conditions. This must have been partly due to the fact that the Kipp solarimeter was placed considerably lower than the tube solarimeter .

However, temperature patterns after placement and subsequent removal of the glass plate suggest an additional influence of the change in effective sky temperature, but could not be separated from the overall increases and decreases in temperature in this experiment.

5.2 APPLICABILITY OF THE RESULTS.

As a consequence of the results one should warn for errors in the use of long tube solarimeters under tropical conditions where a comparison is made between windy open and very calm within crop conditions under high ambient temperatures. The trend of errors from the three sources in the research are likely to be the same although it could only be proved for two sources: high temperature/low air movement conditions and condensation. The third source, a difference in effective sky temperature, was

masked by a larger radiation absorption effect and could only be qualitatively shown. In the N/S orientation the sources of errors accumulate into the same trend with radiation geometry ones (Stigter et. al., 1989a; 1989b).

5.3 RECOMMENDATIONS

The warnings put forward in the report above should be taken into consideration in measurements where tube solarimeters are involved. Further research is needed in the following areas:

1) Quantification of effects of tube orientation coupled with high ambient temperatures on output and response in situations where crops are grown, including such conditions as investigated by Kainkwa and Stigter (Mungai, personal communication).

2) Measuring different amounts of condensation in the tube and quantifying its effects, together with measures to prevent condensation. It is good practice to flush the tubes with dry air before use. Sealing the tube using silicone rubber compound may also be useful.

3) Experiments to quantify the effect of apparent sky temperature on tube solarimeter output without interference of other factors.

4) Further improvements of the interface and the software with a view to making it a stand alone data logger with capabilities to upload and download to either BBC or IBM microcomputers.

BIBLIOGRAPHY

Fristchen, L.J. and Gay, L.W. (1979). Environmental instrumentation. Springer-Verlag.

Bray, A.C., Dickens, A.C. and Holmes, M.A. (1983). The advanced user guide for BBC microcomputer. Cmabridge Microcomputer Center, UK.

Cornwell, K. (1977). The flow of heat. Van Nostrad Reinhold Co. Ltd. London.

Sparrow, E.M. and Cess, R.D. (1980). Radiation heat transfer. McGraw Hill.

Woodward, F.I. and Sheehy, J.E. (1983). Principles and measurements in environmental biology. Butterworths.

REFERENCES

BBC MIS kit manual, 1980. University of York, Electronics Department.

Benedict, R.P. (1969). Transient temperature measurement. In "Fundamentals of temperature, pressure and flow measurement". pp.142 - 155.

Bray, A.C., Dickens, A.C. and Holmes, M.A.(1983) The advanced user guide for BBC Microcomputer. Cambridge Microcomputer center U.K.

Cornwell, K. (1977). Heat flow. Van Nostrand Reinhold Co. Ltd. London. pp. 44.

Corning Ltd., 1981. Catalogue of Labware and Scientific Equipment. Laboratory Division, England.

Delta-T Devices Ltd.,UK. Tube solarimeters manual 1984.

Drake, W.H. (1987). Interfacing the BBC using simple interface kits. ICTP Workshop on micros, Khartoum

Fritschen, L.J. and Gay, L.W. (1979). Radiation . In " Environmental instrumentation ". Springer-Verlag. pp.93-118.

Incropera, F.P. (1981). Fundamentals of heat transfer. John Wiley & Sons, Inc. USA pp. 761-792.

John Fluke Mfg Co. Inc. Seattle, U.S.A. Digital thermocouple thermometer. Instruction manual 1975.

Kipp and Zonen, Netherlands. Solarimeter for outdoor

installation.

Kipyegon (1989). Light sensors. A final year project report. Department of Physics, University of Nairobi.

Lang, A.R.G. (1977). A note on the cosine effect of cylindrical radiometers. J. Agric. Met. 19:391-397.

Monteith, J.L. (1973). Radiation. In "Principles of environmental Physics". Edward Arnold. pp.23-77.

Ng'etich, W.K. (1987). Thermal conductivity measurement using a data logger. A final year project report. Department of Physics, University of Nairobi.

Norris, D. J. (1973). Calibration of pyranometers. Solar Energy 14. pp.99-108.

Pit, J. and Coulson, C.L. ,1987. The interfacing of a portable Infra Red Gas Analyser to a BBC Microcomputer for faster and more convenient processing of field data.

Sciez,G. , Monteith,J.L. and Dos Santos,J.M. (1964). Tube solarimeter to measure light among plants. J. Appl. Ecol. 1:169-174.

Shaw, R.H., G. Kidd and G.W. Thurttell (1973). A miniature three-dimensional anemometer for use within and above plant canopies. Boundary layer Met. 3:359-380.

Sparrow, E.M. and Cess, R.D. (1980). Radiation heat transfer. McGraw-Hill pp.33-80.

Stigter, C.J. and V.M.M. Musabilha (1982). The conserative ratio of photosynthetically active radiation in the tropics. J. Appl. Ecol. 19:853-858.

Stigter, C.J., C.L. Coulson, A. El-Tayeb mohamed, D.N. Mungai and R.M.R. Kainkwa (1989a). Users' needs for quantification in tropical agrometeorology: Some case studies. In: Proceedings of the Fourth Technical Conference on Instruments and observation (TECIMO IV). Instruments and observing methods report no. 35 WMO/TD no. 303, Geneva, 365-370.

Stigter, C.J., C.L. Coulson, D.N. Mungai, R.M.R Kainkwa, A. El-Tayeb mohamed, A.A. Ibrahim, F.S. Mpelasoka and B.I. Abdulai (1989b). Some examples of quantification in tropical agrometeorology for low - resource agriculture in Africa: instruments and on farm research conditions. Proceedings of the Second ICTP/SAPAM workshop on the applicability of Environmental Physics and meteorology in Africa, Addis Ababa University, SAPAM/ICTP, in print

Woodward,F.I. and Sheehy,J.E. (1983). In "Principles and measurements in Enviromental Biology". pp. 174-178. Butterworths.

APPENDIX

SOFTWARE LISTING

```
5 CLEAR
10 DIM A(100),B(100),C(100),D(100),E(100),F(100),G(100),
H(100)
20 *KEY0 RUN ¦¦M
30 CLS
40 PRINT TAB(5,2);"Is your data from the Interface (I),
from disk (D) or you want to exit (Q) ?":S$=GET$
50 IF S$ = "D" THEN PROCread
60 IF S$ = "I" THEN 80
70 IF S$ = "Q" THEN END ELSE 40
80 INPUT "For how long do you want to read data ";N
90 PRINT "Seconds (S), Minutes (M), or Hours (H) ":L$ =
GET$
100 IF L$ <> "M" AND L$ <> "S" AND L$ <> "H" THEN 90
110 IF L$ = "M" THEN N = N*60:GOTO 130
120 IF L$ = "H" THEN N = N*3600
130 CLS
140 M = 0
150 TIME = 0: REPEAT
160 V = TIME
170 I = 1
180 ?&FE62 = 6 :REM Setting the data direction register
(B).
190 REM
200 ?&FE60 = 1
210 ?&FE60 = 0: REM Generate clock signal by outputing 1
and 0.
220 A(I) = ?&FE60: REM Data is read in to the computer.
230 I = I+1: IF I>40 THEN THEN 240 ELSE 180
240 ?&FE62 = 6
245 REM Calculation changing from BCD to decimal
250 B(M) = A(1) + (A(5)*2) + (A(3)*4) + (A(7)*8)
260 C(M) = A(2) + (A(6)*2) + (A(4)*4) + (A(8)*8)
270 D(M) = A(9) + (A(13)*2) + (A(11)*4) + (A(15)*8)
280 E(M) = A(10) + (A(14)*2) + (A(12)*4) + (A(16)*8)
290 F(M) = A(17) + (A(21)*2) + (A(19)*4) + (A(23)*8)
300 G(M) = A(33) + (A(37)*2) + (A(35)*4) + (A(39)*8)
340 IF A(24) = 1 THEN 350 ELSE 390: REM CHECK FOR OPEN
THERMOCOUPLE
350 CLS
360 PRINT "Error ! open thermocouple at channel ";G(M)
```

```
370 PRINT "Check thermcouple or change to another channel
and press any key to continue ":K$ = GET$
380 GOTO 130
390 IF A(38) = 1 THEN 410
400 IF A(36) = 1 THEN 420 :REM check for reading units
410 PRINT "DTT  Reading is ";B(M);C(M);D(M);E(M);".";F(M);
" 'C":GOTO 430
420 PRINT "DTT Reading is ";B(M);C(M);".";D(M);E(M);F(M);
" mV"
430 PRINT "Channel number is ";G(M)
440 IF A(34) = 0 THEN 450 ELSE 460 : REM polarity check
450 PRINT TAB(10,7);"The polarity is     -":GOTO 470
460 PRINT TAB(10,7);"The polarity is     +"
470 IF L$ = "S" THEN 500
480 IF L$ = "M" THEN 510
490 IF L$ = "H" THEN 520
500  PRINT  TAB(10,11);  "Time  is  ";INT((V/100)*100)/100);"
Secs  ":GOTO 530
510  PRINT  TAB(10,11);  "Time  is  ";INT((V/6000)*100)/100);"
Secs ":GOTO 530
520 PRINT TAB(10,11);"Time is ";INT((V/360000)*100)/100);
" Hours  "
530 FOR I = 1 TO 2300: NEXT : REM delay
540 REM
550 M = M+1: UNTIL N = V/100 OR N<V/100
560 PRINT "Do you want to save data to disk (S), send data
to printer (P), restart taking data (B) or exit (Q) ?":W$
= GET$
570 IF W$ = "S" THEN PROCsave
580 IF W$ = "P" THEN PROCprint
585 IF W$ = "B" THEN 5
590 IF W$ = "Q" THEN END ELSE 560
595 END
600 DEF PROCsave
610 INPUT "Name of file to hold data ";D$
620 Y = OPENOUT D$
630 FOR I = 1 TO M
640 PRINT £Y,B(I),C(I),D(I),F(I)
650 NEXT
660 PRINT £Y,M
670 REM
680 CLOSE £Y
690 ENDPROC
700 DEF PROCread:INPUT "Name of file holding data ";H$
710 Y = OPENIN H$
720 INPUT £Y,M
```

```
730 I = 0
740 REPEAT
750 INPUT £Y,B(I),C(I),D(I),E(I),F(I)
760 I = I+1:UNTIL EOF£Y
770 CLOSE £Y
780 ENDPROC
800 DEF PROCprint:PRINT "Set the printer ONLINE and press
any key to continue":Y$ = GET$
810 *FX6,0
820 VDU2
830 PRINT M
840 FOR I = 1 TO M
850 PRINT B(I),C(I),D(I),E(I),F(I)
860 NEXT
870 VDU3:ENDPROC
```

```
730 I = 0
740 REPEAT
750 INPUT £Y,B(I),C(I),D(I),E(I),F(I)
760 I = I+1:UNTIL EOF£Y
770 CLOSE £Y
780 ENDPROC
800 DEF PROCprint:PRINT "Set the printer ONLINE and press
any key to continue":Y$ = GET$
810 *FX6,0
820 VDU2
830 PRINT M
840 FOR I = 1 TO M
850 PRINT B(I),C(I),D(I),E(I),F(I)
860 NEXT
870 VDU3:ENDPROC
```